A review on mechanical considerations for chronically-implanted neural probes

Aziliz Lecomte, Emeline Descamps, Christian Bergaud

TOPICAL REVIEW

A review on mechanical considerations for chronically-implanted neural probes

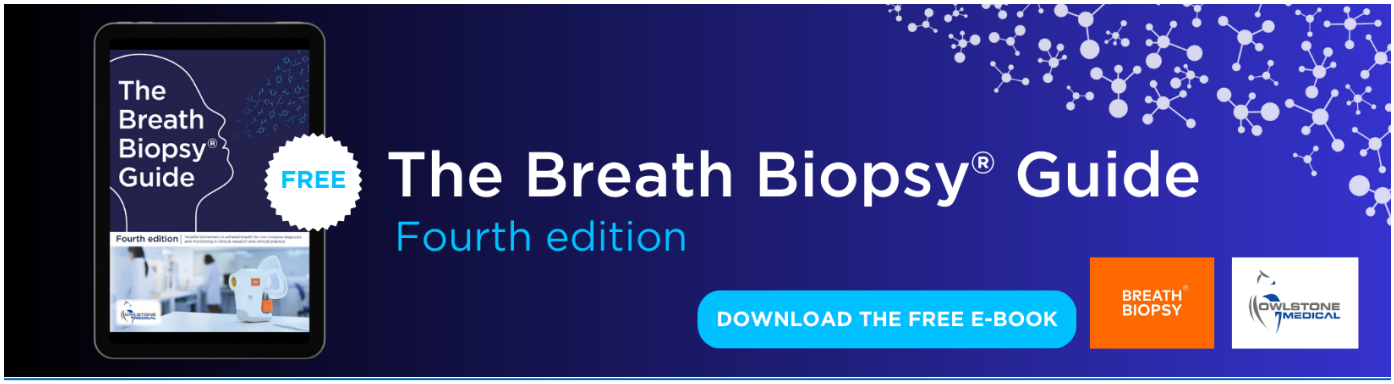

IOP Publishing Journal of Neural Engineering

J. Neural Eng. **15** (2018) 031001 (21pp) https://doi.org/10.1088/1741-2552/aa8b4f

Topical Review

A review on mechanical considerations for chronically-implanted neural probes

Aziliz Lecomte, Emeline Descamps and Christian Bergaud

LAAS-CNRS, Université de Toulouse, CNRS, Toulouse, France

E-mail: alecomte@laas.fr and christian.bergaud@laas.fr

Received 30 March 2016, revised 29 June 2017
Accepted for publication 8 September 2017
Published 5 March 2018

Abstract

This review intends to present a comprehensive analysis of the mechanical considerations for chronically-implanted neural probes. Failure of neural electrical recordings or stimulation over time has shown to arise from foreign body reaction and device material stability. It seems that devices that match most closely with the mechanical properties of the brain would be more likely to reduce the mechanical stress at the probe/tissue interface, thus improving body acceptance. The use of low Young's modulus polymers instead of hard substrates is one way to enhance this mechanical mimetism, though compliance can be achieved through a variety of means. The reduction of probe width and thickness in comparison to a designated length, the use of soft hydrogel coatings and the release in device tethering to the skull, can also improve device compliance. Paradoxically, the more compliant the device, the more likely it will fail during the insertion process in the brain. Strategies have multiplied this past decade to offer partial or temporary stiffness to the device to overcome this buckling effect. A detailed description of the probe insertion mechanisms is provided to analyze potential sources of implantation failure and the need for a mechanically-enhancing structure. This leads us to present an overview of the strategies that have been put in place over the last ten years to overcome buckling issues. Particularly, great emphasis is put on bioresorbable polymers and their assessment for neural applications. Finally, a discussion is provided on some of the key features for the design of mechanically-reliable, polymer-based next generation of chronic neuroprosthetic devices.

Keywords: chronic implantation, neuroprosthetic devices, brain mechanical properties, stress relief, insertion methods, flexible polymers, biomaterials

(Some figures may appear in colour only in the online journal)

1. Introduction

Neural interfaces aim to bridge the brain to the outside world, through the recording or stimulation of neural activity. As an example, brain–computer interfaces (BCIs) intend to restore or by-pass functional skills for patients with paralysis, motor dysfunction or limb loss [1]. A variety of devices can be used for interfacing with the central nervous system, where their invasiveness is directly linked to the application of the BCI. Macro-electrodes on the scalp can record slow (~100 Hz) variations of brain waves, and might be used for simple computer transduction, such as spelling devices [2, 3]. On the other hand, implantable electrodes are able to detect high quality field potentials and single neuron activity with great temporal resolution (0.2–7 kHz) [4], which could be used to control more complex external devices, such as a robotic hand [5, 6]. Moreover, uses for implantable devices are emerging in the treatment of numerous diseases, from Parkinson's deep brain stimulation to dystonia and depression [7]. While implantable electrodes have been widely used for neurophysiological

aims, the turn toward chronic implantation has brought many issues that are yet to be addressed. Unstable electrical recordings over time vary with body acceptance and implant material lifetime. In the case of stimulating devices, signal amplitude is often increased to get around the scarring zone. The implantation of a foreign body in the brain involves a mechanical and biological trauma that brings device migration and encapsulation, eventually resulting in impedance increase or even loss of functionality [8, 9]. Metal corrosion and degradation of passivation layers also play a great role in device failure over long periods of time [10]. To increase device acceptability, biocompatibility and material life time have become areas of interest [4], as well as insertion conditions and design optimization [11, 12].

Historically, silicon has been extensively exploited in neuroprosthetics. While an insulating layer offers an improvement in electrode viability, other parameters are yet to be taken into account. The mechanical mismatch between a standard silicon probe (modulus 150–170 GPa) and the surrounding tissues (modulus 3–100 kPa) still prompts a great deal of strain. Indeed, the brain micromotions-respiration, vascular pulsatility and head movements, induce displacements in the order of tens of microns around the silicon or metal shank, which leads to an enhanced mechanical stress around the shank [13]. In this sense, theoretical modeling work showed that flexible implants should absorb parts of these micromotion forces, especially in the x and y directions [14]. Following this lead, one of the emergent approaches is the use of flexible, polymer-based neural shanks that partially relieves the stress between the soft tissues and the implanted device [14, 15]. But designing a neural probe that mechanically matches brain tissues is demanding, especially considering that, to this day, there is no consensus over the ideal form such a probe should take. Mechanical compliance is often associated with flexibility and Young's modulus, when other parameters need to be taken into account, such as insertion footprint and device tethering to the skull. A probe too thin or too flexible, though ideal for a stress-reducing implant, would be impractical to handle, and would eventually tear, deform and break. Furthermore, this compliant probe should be able to be implanted in the brain and reach a targeted region without failing. Numerous studies focused on the best way to overcome this stiffness/flexibility paradox for a large range of applications, yet no miracle solution is standing out.

The mechanical considerations for chronically-implanted neural probes sets the background for this review. In the first section, we introduce the notion of strain in the context of intracortical probes, along with the strategies to achieve better mechanical compliance with the surrounding environment. One can focus on the addition of a hydrogel coating or the turn towards polymeric implants to reduce the stress around traditional hard devices, on implant geometry, on device fixation mode, or a combination of these strategies. A new generation of soft, thin, floating implants could represent substantial advances in the acceptance and reliability of intracortical prosthetic devices.

Paradoxically, as researchers strive to achieve mechanically-mimicking implants, these very same devices often fail during the implantation procedure: they are too thin or too flexible to withstand insertion forces and generally fail while trying to make their way into the tissue. The second section is dedicated to the insertion strategies that have been developed over the years to assist implantation of compliant devices. After an introduction on insertion mechanisms, these strategies are described and discussed, such as the use of a retractable tool or bioresorbable polymers.

Finally, certain mechanical considerations for intracortical probes and their engineered solutions is discussed. The influence of insertion conditions and footprint, the enhancement of device interfaces through bioactive features and possible coating formations inspired from the tissue engineering field, are potentially marking the path towards a new generation of engineered intracortical implants that are reliable long term.

2. How to achieve stress relief for chronic implantation

2.1. Chronic stress at the probe/tissue interface and compliance

As stated in the introduction, the main hypothesis is that the mechanical strains that arise around the implant site represent one of the leading factors responsible for the sustained tissue response [14, 15]. The pulsatile micromotions issued from respiration and cardiac pace create a stress at the probe/tissue interface, consequently aggravating body inflammation. In rat brains, these micromotions are on the order of tens of microns for respiration-induced pressure and 0.2 μm due to cardiac-induced pressure [13] (figure 1(A)). Finite element stimulation shows that tethering forces induce elevated strains, located principally at both tips of the probe [14] (figure 1(B)).

Targeting stress-relief for chronically implanted intracortical probes presents with many aspects. It is generally accepted that a device that matches most closely to the surrounding tissues would have a better chance of being accepted [14, 18, 19]. This mechanical mimetism, also known as compliance, is often mistakenly associated with material flexibility. Compliance represents the ability of a system to deflect upon axial forces brought on it by the surrounding tissues, and therefore is closely linked to the buckling force described by Euler's formula

$$F_{\text{buckling}} = \frac{\pi^2 I_x E}{(KL)^2} \tag{1}$$

where F_{buckling} is the buckling force, E is the beam Young's modulus, L its length (dimension along the z axis) and K the beam effective length factor, whose value depends on the beam fixation. The moment of inertia I_x along the x axis depends on the shape and dimension of the beam cross-section. In the case of a rectangular beam, it is equal to $I_x = \frac{ab^3}{12}$, where a is the beam thickness (dimension along the y axis) and b its width (dimension along the x axis, where the buckling occurs).

Therefore, the compliance is a function of structure, while flexibility (elastic modulus) is a function of material [20]. As an example, for the same length, width and fixation mode, a 20 μm-thick Parylene beam (E~3 GPa) would have approximately the same compliance as a 5 μm-thick silicon beam

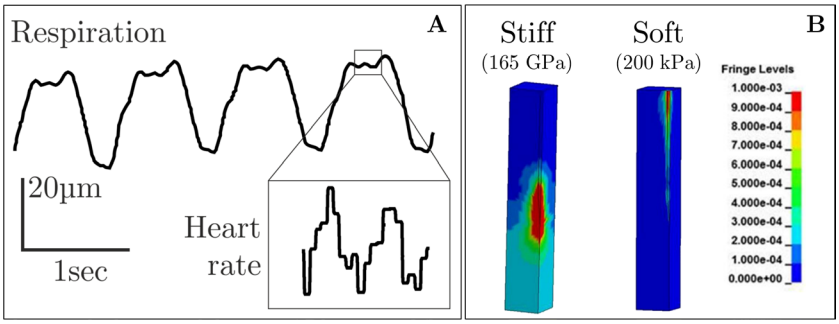

Figure 1. (A) Typical brain micromotion pressures induced by respiration and vascular pulsatility (heart rate) in a rat brain (© (2005). © IOP Publishing Ltd. All rights reserved. IEEE. Reprinted, with permission, from [13] and reproduced from [16]. © IOP Publishing Ltd. All rights reserved.). (B) Modeled strain distribution at the probe/tissue interface using a micromotion displacement of 4 μm for both a silicon probe (165 GPa) and a soft probe (200 kPa). Results indicate elevated strain for the silicon probe, especially at the tip (reproduced with permission from [17]. CC BY 4.0.).

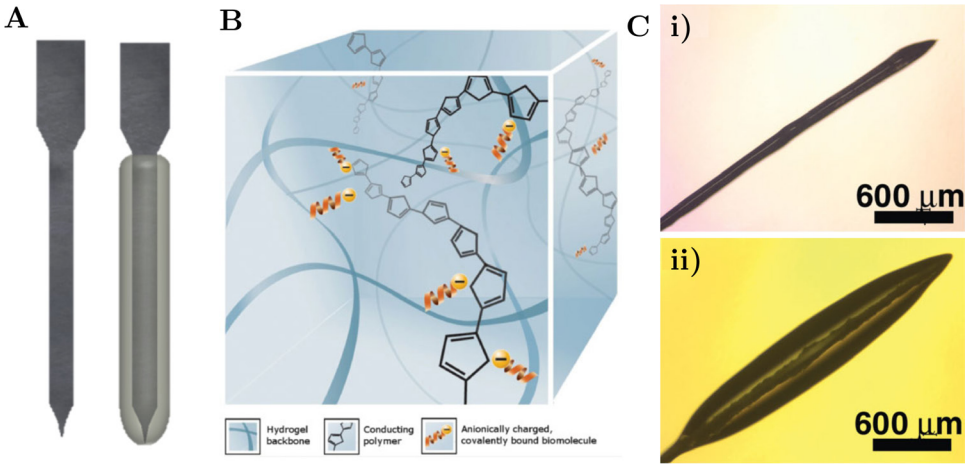

Figure 2. Examples of hydrogel coatings for neuroprosthetic devices. (A) Solid 300 μm-wide silicon shank before (left) and after (right) multiple dip-coating in sodium alginate hydrogel (400 μm-thick) used to study the impact *in vivo* of a permeable coating (reprinted from [21], copyright (2015), with permission from Elsevier). (B) Ideal schematic of a hydrated conductive hydrogel with covalently bound bioactive agents (reproduced with permission from [22] John Wiley & Sons. Copyright © 2012). (C) Side view optical micrographs of a neural electrode after coating with dexamethasone-loaded electrospun nanofibers and alginate hydrogel in (i) dehydrated state and (ii) hydrated state, showing the increase of mechanical footprint due to hydrogel swelling (reproduced with permission from [23] John Wiley & Sons. Copyright © 2009).

(E~200 GPa). Consequently, to achieve better compliance, one or several strategies can be chosen:

(i) reduce the effective elastic modulus of the material. This can be done, for instance, either by using low-modulus coatings such as hydrogels, or by fabricating the device from flexible polymer materials,
(ii) adjust the dimensions of the probe, that is to say, reduce the cross-section or increase device length,
(iii) loosen the device fixation to the skull.

2.2. Hydrogel coatings around stiff shanks

Silicon neural implants remain the most widespread technology, with the huge success of Utah-like or Michigan arrays [24]. It allows integration of circuitry components on the shaft, also known as CMOS-based neural probes [25, 26]. Indeed, high numbers of electrodes over a single shank are desirable to investigate complex neural networks and CMOS technology allows us to overcome the spacing and width limitations of parallel leads defined by lithography. Therefore, manufacturing active high-density probes with *in situ* amplification can be performed on a silicon substrate, retaining focus on this traditional microelectronic substrate.

Silicon Young's modulus is in the range of 200 GPa, well above that of brain parenchyma (figure 3). A coating might mediate the mechanical difference between soft tissue and hard devices (figure 2(A)). Recently, Sridharan *et al* showed that bare silicon shanks (15 μm thick, 200 GPa) coated with a compliant nanocomposite material (coating 15 μm thick, 12 MPa) resulted in a device with an average of 49–70 GPa, which does not significantly lower the overall stiffness of the probe. However, *in vivo* brain micromotions-induced stress amplitude was similar for coated devices and for compliant structures (127 μm), which suggests that parameters, other than pure moduli, play a key part in stress reducing, for example surface adhesion properties [15].

Hydrogels are polymers extensively used in tissue engineering, with tunable physical and chemical properties dependent on cross-linking networks. Hydrogels from natural materials such as fibrin [27], collagen [28] and alginate [21, 23, 29], promote cellular interactions that result in increased body acceptance. On the other hand, the mechanical properties of

synthetically-polymerized hydrogels like polyvinyl alcohol (PVA) [30] and polyethylene glycol (PEG) [31] are easier to control [32]. Besides enhancing mechanical mimetism, hydrogel systems may benefit from modifications to incorporate covalently-bound bioactive agents, that promote neuritic outgrowth and cell density around the probe [28, 30, 33]. Very often, hydrogels are blended with conductive polymers (CP) such as poly(3,4-ethylenedioxythiophene) (PEDOT) and poly(pyrrole) (PPy) [34, 35], providing enhanced electrical characteristics while insuring reduced stiffness [22] (figure 2(B)). CP electropolymerization tends to reduce electrode impedance and increase the charge transfer capability, which makes them desirable to enhance electrical interfaces for both intracortical recording and stimulation [32, 36]. In this sense, conductive hydrogels combine the mechanical approach of hydrogels while retaining superior electrical properties when compared with traditional metal electrodes [22, 37]. More information on organic coatings are available in specialized reviews [4, 32, 34].

On the negative side, swelling of hydrogel-based polymers in the hydrated state can be considerable, consequently pushing target neurons away from the electrode [38] and increasing the risk of delamination (figure 2(C)). Thick alginate coatings (80 μm) have been shown to increase loss of recording functionality and decrease SNR in the guinea pig auditory cortex [38]. The choice of cross-linker type and cross-linking density should be studied to define the appropriate mechanical stability of hydrated states [39], and the stress and brain tissue deformation from hydrogel hydration should be evaluated. Finally, whereas many hydrogels have been investigated in the tissue engineering field, and many excellent reviews focus on conductive hydrogels for biomedical applications [4, 32, 34, 40], only a few studies have been carried out for intracortical applications [32].

2.3. Choice of a flexible substrate

2.3.1. Flexible substrates. The most obvious way to reduce the stress at the probe/tissue interface is to build devices out of softer materials, such as flexible polymers. As their Young's modulus approaches that of cerebral tissues, the mechanical mismatch will be significantly reduced, along with the stress amplitude [15].

Flexibility scaling remains an unresolved issue. The designation of 'flexible' has not yet been universally defined, and the polymers used as soft substrates for neural applications involve a wide range of Young's moduli, as seen in figure 3. This lack of universal terminology might be misleading. For instance, a recent study showed that neural immune cells respond to mechanical cues *in vitro* as well as *in vivo*, where the 'stiff' probes used in the study had an elastic modulus of 10–30 kPa and 'flexible' probes a modulus of 100 Pa [45]. On the other hand, tens and maybe hundreds of studies imply that polyimide and Parylene C are 'soft' materials for neural applications, yet their modulus reaches 2–5 GPa, that is to say 100 000 times stiffer. For the sake of understanding, we will hereinafter refer to 'soft' or 'flexible' polymers those with an elastic modulus in the order of the GPa.

Several polymers have been tested as soft substrates for intracortical electrodes; Parylene [46], polyimide [43] and

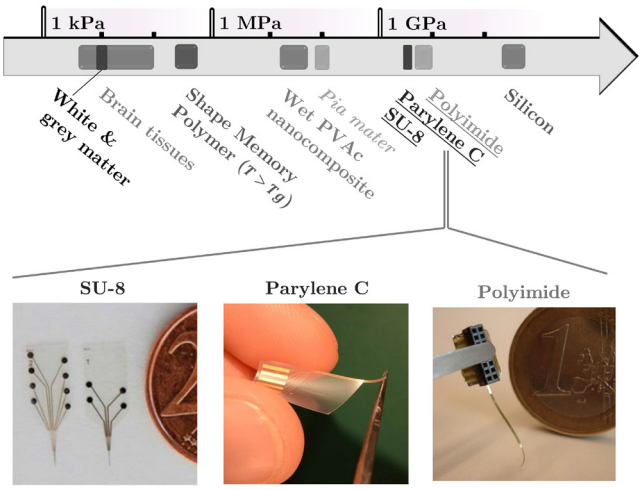

Figure 3. Schematic scaling representing the mechanical properties (Young's modulus) of both brain tissues and neural probe substrate along with photographs of the most common flexible substrates (Parylene C (reproduced from [41] © IOP Publishing Ltd. All rights reserved), SU-8 (reproduced from [42] with permission of The Royal Society of Chemistry.) and polyimide (reprinted from [43], copyright (2008), with permission from Elsevier))—freely adapted from [44] (Taylor & Francis Ltd. http://tandfonline.com).

SU-8 [47] being the most popular [48]. Typically, polymer probes dimensions are on average 100–500 μm wide, 10–30 μm thick, with a length varying from 1 to 6 mm [43, 49–51]. For more information on the properties of each polymer, the reader should refer to Weltman *et al* [52].

Parylene (Poly(p-xylylene)) has proven to be a prominent choice [51, 53–55] due to its lower mechanical properties (Young's modulus 2.76 GPa), highest standard of biocompatibility (ISO 10993 USP, Class VI biomaterial) and chemical inertness. It is deposed through chemical vapor deposition (CVD) at room temperature under vacuum, which makes it easy to integrate into classic microfabrication techniques. The resulting film is transparent, pinhole-free, conformal and provides excellent water-barrier properties. One of the drawbacks of Parylene is its low adhesion to many substrates, especially metals [56], while adhesion in wet environments is one of the most crucial properties for implant survival [57]. Hermeticity and layer adhesion of Parylene devices have been tested *in vitro* through ageing tests and peeling assays [56–59]. Recently, *in vivo* studies during one to 12 months in rats and mice have shown little material degradation, correlated with stable recordings and minimal glial scarring [60–62].

Polyimide (PI) is also chemically inert, electrically insulating and compatible with microelectronic processes [63]. Its patterning can be achieved through direct photolithography (photosensitive) or with a dry etching step (non-photosensitive) in $CF_4 + O_2$ plasma. Kapton (PMDA-ODA) is one of the most commonly used non-photosensistive types, but is sensitive to humidity in the long run [64]. The BPDA-PPD polyimide was successfully used in neural implants [65] and have been tested *in vitro* in both soaking and ageing tests [66]. It is important to note that PI has not yet been approved by the US Food and Drug Administration (FDA), but its biocompatibility in animal models is well documented [66, 67].

SU-8 is a transparent epoxy based negative photoresist that can be patterned in thick layers with high-aspect ratio, and has found utility in drug delivery devices or as a waveguide for optogenetic studies [42, 68–70]. However, SU-8 biocompatibility in the long run is still doubtful. A study by Kotzar and coworkers performed *in vitro* and *in vivo* tests on SU-8 devices according to ISO 10993 standards, and expressed doubts on SU-8 resistance to sterilization and on possible irritations.

Thermo and chemo-responsive polymers are also primarily considered for such application, for their elastic modulus drops in physiological fluids [8]. In the dry state, their elastic modulus is indeed in the order of the MPa, which matches most closely that of the brain. For instance, the Capadona group developed a new class of chemoresponsive polymers, a poly(vinyl acetate) nanocomposite (PVAc) with a structure that mimics that of sea cucumber dermis. However, PVAc is not compatible with traditional microfabrication processes, and electrical intregration on this substrate has yet to be shown [71].

Other flexible devices made of liquid crystal polymers [72], benzocyclobutene (BCB) [73] or carbon nanotubes [74] are also starting to emerge, but have a long way to go before being considered as actual substrates for chronic purposes.

2.3.2. Elastic substrates. Stretchable devices, such as polydimethyl siloxane (PDMS) and relatives, embody an alternative for strain-relief in subdural implantation, as the device is dynamically adaptive. PDMS is widely used in microfluidic technologies, and has high viscoelasticity with a Young's modulus that can be slighlty altered depending on the curing agent and temperature. A comparative study by Minev and coworkers has recently shown that a polyimide implant induced a pronounced flattening of a simulated spinal cord, whereas a soft, elastomeric implant showed great compliance when the model was bent, avoiding local compression along the hydrogel cord [75]. Applied to intracortical probes, elastomeric substrates might be useful for a better compliance when consequent strain is to be expected, for instance in curved or dynamic areas. Though PDMS exists in medical class, that meets both USP class VI and ISO 10993, it has been reported that the curing agent might be toxic [76]. Solvent residues can indeed infer cytotoxicity [8], and extra care should be taken in the curing and sterilization steps.

2.3.3. Density. Material density also has a role to play. In a study by Lind *et al*, low-density probes (1.35 g cm^{-3}) produced very little glial scarring, compared to high-density probes (21.45 g cm^{-3}) with the same shape, size and isolating material [77]. According to the authors, since brain tissue density is estimated at 0.99 g cm^{-3}, a large difference in density leads to inertial forces when the implanted animal changes speed or direction. The reduction of glial scarring through material changes is a more global approach than the reduction in Young's modulus, and biomimetic approaches need to incorporate more material parameters to increase implant acceptability.

2.3.4. Concerns on polymer-based implants. Many issues have been reported for polymer implants, for instance the difficulty in integrating them into reliable packaging [8, 52]. The main issue with polymeric implants is the long-term reaction to a water-based environment [8], which have often been shown to fail within months as a result of polymer swelling and layer delamination [20].

Delamination. The passivation layers and insulation coatings commonly incorporated in microelectrodes may degrade over time. This phenomenon is exacerbated as passivation layers are often composed of polymeric chains, that tend to swell and lift in physiological conditions [10]. Whenever a polymer is used as a passivation layer, the coating must be flawless, void-free, and stable with good adhesion that is impermeable for ions. Thermoplastic materials such as Parylene C can be thermally treated at a temperature greater than the glass transition point during or after fabrication. The proportion of crystallinity versus amorphousness in the structure is increased, and bonds between the different layers are formed [78, 79]. Layer adhesion can also be promoted using adhesion promotors (e.g. Silane A-174) [56] or surface modifications (e.g. plasma, UV ozone) [41, 64, 80]. Finally, residual stresses from processing (thermal, mechanical, hygroscopic) can lead to increased deadhesion of the layers composing the neural device [64].

Swelling. Swelling of polymers increases device volume, which induces pinching of nearby blood vessels and capillaries, leading to a deporter injury beyond the initial injury site [20]. Besides, water uptake leads to film cracks and hole formation that eventually affects the device's mechanical and electrical properties. Atomic-layer-deposited aluminum oxide or silicon oxide on top of the encapsulation layer [58, 81, 82] may be used to create a moisture barrier, and permeabilization might alter surface water affinity [21].

2.4. Implant dimensions

Reducing substrate thickness and width undoubtedly leads to greater compliance, as the buckling force is significantly reduced, so that the resulting device fits more closely to the tissues. Thickness reduction represents an opportunity for silicon or tungsten-based implants, to match more closely to the surrounding tissues even with a high elastic modulus. Silicon or tungsten wire implants usually have a small diameter, but only one electrode is available per shaft [24, 83]. Ultra-thin silicon shanks can be obtained using boron or SOI etch-stop techniques, with a thickness in the range of 5–20 μm [24, 26, 84]. Commercial NeuroNexus silicon probes are for instance available with 15 or 50 μm thickness, yet extra care should be taken when dealing with these thin shanks: thin layers of brittle material increase the occurrence of shank fracture.

Overall, the question of scale and limits is yet to be studied as a function of purpose to define how thin is thin enough. From a mouse brain to a human brain, it seems clear that the size requirements are not even. In terms of length for instance, the device needs to be designed to target a specific brain region for a specific species, therefore designing a 'thin' probe for a hippocampal study on mouse brain (1.2 mm in depth [85]) or a neurostimulator for human thalamic nucleus (~40 cm [86]) will definitely not have the same requirements. The same argument goes for shank width: most of the surface is covered

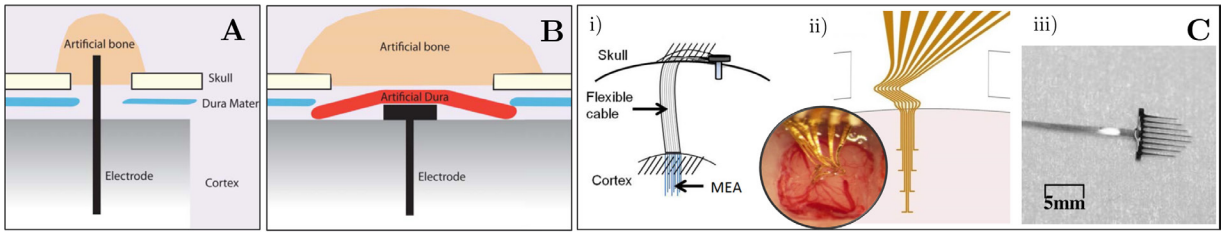

Figure 4. (A) Tethered, (B) untethered and (C) alleviated intracortical fixation mode. (A) Usual implants tethered to the skull exacerbate mechanical tearing and relative micromotions, which results in increased inflammation over the long term [87] (© 2011 Thelin *et al*). (B) Untethered implant can be ensured by adding artificial *dura* on top of the implant, separating the implant from the skull ((A) and (B) reproduced with permission from [87] © 2011 Thelin *et al*), but are hard to implement with traditional packaging and connection techniques. (C) (i) Alleviated fixation can be achieved via a flexible cable between a traditional silicon MicroElectrode Array (MEA) and the fixation on the skull (reproduced with permission from [88] © 2013 Sankar, Sanchez, McCumiskey, Brown, Taylor, Ehlert, Sodano and Nishida). (ii) Schematic and picture of the insertion *in vivo* of a 'Z-shape' implant, where the design is meant to match that of brain structures to enable some stress relief on the electrodes (reproduced with permission from [89] © 2015 Agorelius, Tsanakalis, Friberg, Thorbergsson, Pettersson and Schouenborg). (iii) A silicon array integrated with a Parylene flexible cable, meant to relief possible mechanical damages due to relative motion between the brain and the skull (© (2008) IEEE. Reprinted, with permission, from [90]).

by connection leads, therefore width is partially limited to the number of electrodes needed [24]. Consequently, neuroprosthesis dimensions are highly application-driven, and downscaling implant size is limited to (1) the targeted intracortical layer (2) human or animal model (3) the number of needed electrodes and (4) sufficient mechanical holding for proper handling without breakage.

2.5. Skull tethering

The stress at the implant/tissue interface can be exacerbated as a result of mechanical tethering of the device to the skull [91]. Studies have shown that compared with untethered and freely floating implants, skull-anchored microelectrodes elicited significantly greater macrophage/microglial activation and increased astrogliosis [87], which are signs of increased inflammation (figures 4(A) and (B)). *In vivo* in rats, hollow fiber membranes were found to prompt greater immunoreactivity when they were transcranially implanted than when they were implanted intraparenchymally, without skull attachments [92]. However, it is hard to implement a floating-like packaging with a reliable connection for recording or stimulation of the device, especially in the long term.

Instead of avoiding skull tethering altogether, the integration of a flexible cable might be able to relieve part of the strain by decreasing the relative motion between the brain and the skull [88, 90, 93] (figure 4(C)). Upper implant geometry may be designed to match anatomic architecture of the skull. Examples include the 'Z-shape' structure proposed by Agorelius *et al* [89] or the serpentine shape suggested by Sankar *et al* [88], which provide a way to absorb the majority of the motions between the brain and the skull. These are beneficial strategies that should receive increased attention in the future.

In this first section, we discussed several biomechanical mimetism approaches to ensure a better intracortical probe compliance in the surrounding tissues. This is a substantial topic for research that targets chronic reliability of neuroprosthetic devices. Ironically, the very same parameters that are optimized for a maximal compliance, prevent the device from being able to penetrate the brain. Soft, thin, floating implants indeed tend to fail to penetrate the *pia mater* and reach their location goal. The buckling of such implants has been highly discussed in the literature, leading to a strong focus over the last ten years to find the best way to obtain a rigid electrode during surgical insertion, while maintaining its flexibility once positioned in the cortex.

3. How to insert these compliant devices

3.1. Insertion mechanisms

3.1.1. Surgical considerations. For surgical implantation in the cortex, the skin needs to be incised and a craniotomy performed to allow access to the meninges. The *dura mater* is then punctured and the *pia mater* is revealed. The *pia mater* consists of a fibrous impermeable membrane that retains cerebro-spinal fluid. With an elastic modulus reaching 70–100 MPa, it is much stiffer than the white and gray matter underneath [12, 94, 95], and can be nicked for easier implantation. Collagenase has been proposed in the literature as a structure breakdown for the collagen present in the *pia mater*, therefore allowing for easier implantation with minimum dimpling [96, 97].

3.1.2. Agar models of brain tissues. A common method to assess insertion ability is to perform insertions in a brain phantom. Agar gels of different concentrations are often used as tissue phantoms, and more particularly gel at 0.6% in DI water. At this concentration, the agarose gel has an elastic modulus of 10 kPa, a value similar to white and gray matter of the brain [56, 98]. This brain phantom has been widely used as a model of implantation for gray and white matter [99], though it does not take into consideration brain anisotropy. The *pia mater* is rarely considered for such a model, probably because flexible probes have little chance of penetrating it [100], and so puncturing is commonly applied.

3.1.3. Insertion model. From an ideal mechanical point of view, a system may be implanted if the maximum compression force it can withstand before bending (called 'buckling force') is higher than the minimum force required for insertion in the soft tissues (called 'the insertion force') (figure 5).

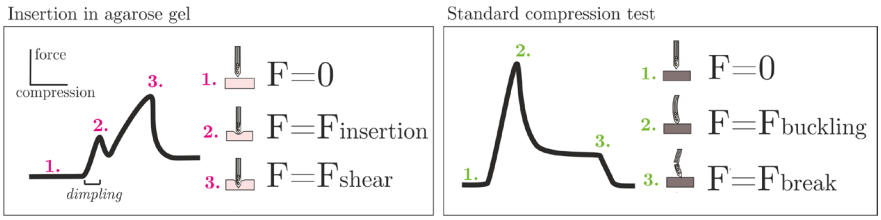

Figure 5. Representative force versus compression curve for a single neural probe compressed (a) in agarose gel 0.6% mimicking brain tissues and (b) against a hard substrate. (a) The compression force will increase as soon as the probe touches the gel surface (1) , and experience a drop (2) when the probe is inserted. The corresponding compression value corresponds to probe dimpling. After being inserted, the probe will cause increasing shear forces as it makes its path into the gel (3)—(b) The compression force increases (1) until the probe starts buckling (2). Ultimately, the compression leads to probe breaking (3). Diagram not to scale.

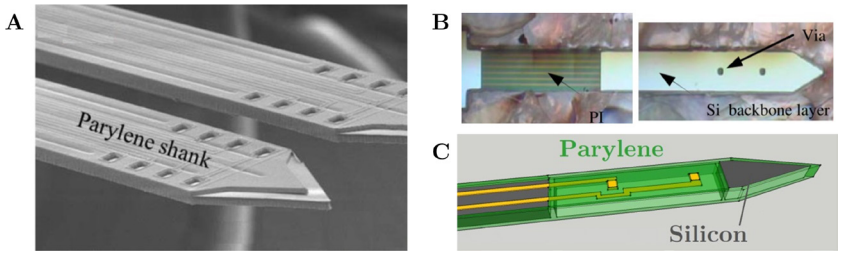

Figure 6. Integrated stiff support for polymer-based neural probes. (A) SEM image of a Parylene probe with integrated vertical stiffeners (© (2011) IEEE. Reprinted, with permission, from [109]). (B) Microscopic image of a thin 5 μm thick silicon backbone layer on a polyimide probe (reproduced from [63] © IOP Publishing Ltd. All rights reserved). (C) Schematic of the hybrid silicon-Parylene C probe with a locally flexible region (reprinted from [110], copyright (2014), with permission from Elsevier).

The buckling force equation viewed in the Euler equation of the previous section is reproduced below.

$$F_{\text{buckling}} = \frac{\pi^2 I_x E}{(KL)^2} \tag{2}$$

The insertion force for white and gray matter is commonly estimated to be around 0.5–2 mN [101–104]. However, from a practical point of view, insertion forces in agarose gel can reach up to 10–50 mN before penetration [41, 71, 100]. Depending on tip shape, implant size, material used and insertion speed, some dimpling is to be expected [11, 105]. Low insertion force and dimpling are not the only parameters to take into account: the maximum shear force the brain will endure along the insertion track is also represents a major concern (figure 5), and highly depends on the depth of insertion [106].

A study by Ruther *et al* showed significant changes in insertion and retraction forces for silicon, glass, polyimide and tungsten probes with varied shapes [100]. In that study, the 460 μm-wide, 10 μm-thick probe was able to sustain insertion in agarose gel, but could not undergo pial insertion *in vivo*. Generally, flexible neural probes have shown to barely withstand implantation [107].

First studies recount the use of extra tools such as a scalpel or a tungsten wire to create incisions meant to match the shaft spacing pattern before actual probe insertion [108], but this induces greater insertion trauma. For the last ten years, strategies have emerged to overcome this flexibility/stiffness paradox. The most common strategies are:

(i) defining a probe that is just hard enough to withstand implantation, or with both rigid and flexible regions,
(ii) using a retractable tool to assist insertion,
(iii) chosing softening materials as probe substrates,
(iv) integrating stiff but bioresorbable polymers on the probe that dissolve in the tissues after implantation.

3.2. Permanent electrode support and hybrid designs

A reasonable approach is to find a compromise between a compliant probe and a probe that is able to withstand implantation. This can be achieved, for instance, with certain tailoring of the probe design: engineered improvements on a Parylene C-based probe with different thicknesses of the material slightly increases the buckling force up to 1.3 mN [109] (figure 6(A)). On the other hand, hybrid silicon/compliant polymer devices are consistent with a simple yet efficient strategy to achieve this compromise. Lee and coworkers first suggested a 5–10 μm silicon backbone enclosed to a polyimide-based probe, multiplying the device Young's modulus by ten (2.8 GPa for a polyimide probe, 31 GPa with a silicon backbone) [63] (figure 6(B)). Recently, a solid silicon/hollow Parylene C tube hybrid design provided an adjustable buckling force of up to 500 mN, thus allowing enhanced insertion in the brain while maintaining reasonable flexibility [110] (figure 6(C)).

The addition of a permanent rigidifier might be considered counterproductive, for the strain relief it brings to cerebral tissues is questionable. In our opinion, the relationship between device compliance and foreign body response needs to be studied in depth before we can consider hybrid systems as suitable candidates for chronic implantation.

3.3. Removable aid

A rigid backbone or shuttle can also be temporarily attached to the compliant device and removed afterwards. For instance, the

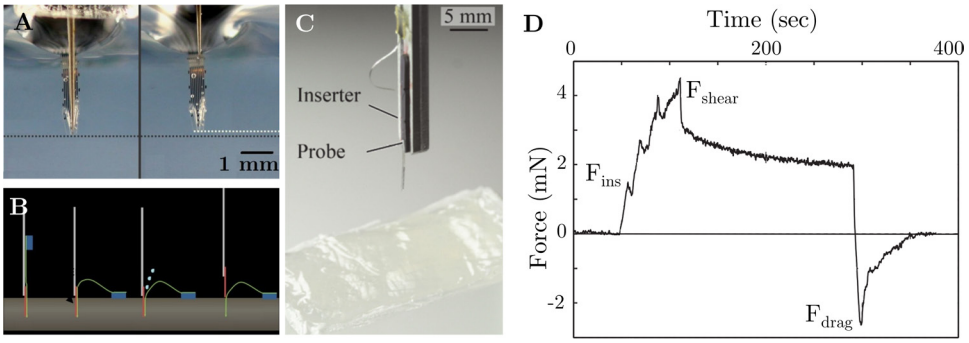

Figure 7. Use of a removable prop extracted after insertion of the flexible device. (A) *In vitro* insertion in agarose gel of a Parylene C probe using a tool nested in the hollow tip (reproduced from [53] © IOP Publishing Ltd. All rights reserved.). (B) Schematic frames of insertion of a silicon stiffener attached to the probe using polyethylene glycol (PEG) as glue, and subsequently extracted after implantation via addition of PBS (© (2012) IEEE. Reprinted, with permission, from [111]). (C) Photograph of the insertion setup for a silicon probe with large sections replaced by a 11 μm-thick polyimide ribbon (© (2015) IEEE. Reprinted, with permission, from [112]). (D) Example of force measurement in a rat brain showing that the retraction force (F_{drag}) is almost the same amplitude as the insertion shear force (F_{shear}) (adapted and reproduced from [106] © IOP Publishing Ltd. All rights reserved.).

shuttle can be separated from the implant through the customization of the probe/shuttle interface. Through a hydrophilic self-assembled monolayer, the two parts adhere electrostatically and separate when in contact with water. Using this technique, Kozai and Kipke showed preliminary results of 8.5 mm deep insertion of a 12.5 μm-thick, 200 μm-wide polyimide-based probe [113]. However, the two surfaces have a high chance of undergoing sliding when surgically manipulated. Resorbable polyethylene glycol (PEG) as a temporary glue guarantees a more reliable adhesion [111, 112, 114] (figures 7(B) and (C)). PEG is a highly biocompatible, fast-degrading polymer, that dissolves quickly with the addition of water. The shuttle can also take the form of a cylindrical needle or a hollow tip where the device to be implanted remains shielded inside [53, 115] (figure 7(A)) and vice versa: the needle can be placed inside a tube-shaped probe [116]. Surprisingly enough, many studies have relied on wide tungsten wires or rods with rather large cross-sections [112, 114, 116, 117]. Silicon for instance, would be more suitable. It can be micromachined in specific dimensions using standard microfabrication techniques, thus creating a particular shuttle design with a minimal cross-section (thickness <100 μm) [111].

One of the challenges of these techniques is to develop a strong, well-aligned coupling between the flexible probe and its rigid support. It is essential to have precise control over support/implant adhesion: a premature dissociation would result in incorrect electrode placement in the brain, and a bond too strong would subsequently prevent the probe from being released. The retraction itself is intricate: the probe tends to withdraw upwards with the retraction force [53, 111] which can be problematic for precise implant positioning. In addition, the retraction force, also referred to as 'drag' force, is on the same order of magnitude as the insertion shear force [100, 106] (figure 7(D)), thus retracting a support would theoretically double the mechanical stress of insertion.

3.4. Mechanically-adaptive substrate

As introduced in the previous section, several smart polymers can adjust their mechanical properties upon different classes of stimuli, such as light, temperature, humidity, etc [44, 120]. A thermally reactive copolymer made of methyl acrylate (MA) and isobornyl acrylate (IBoA) cross-linked with PEG diacrylate was presented as a highly customizable neural probe substrate. The device thus obtained was able to soften from a Young's modulus of 700 MPa down to 300 kPa, 24 h post-insertion [121]. In this structure, the rapid water uptake is a predominant factor in probe softening, which might prove inconvenient for the stability of electrical features. A thiol-ene/acrylate substrate also showed a drop in modulus from 1 GPa to 18 MPa upon exposure to physiological conditions, and succeeded in recording neural activity from the primary auditory cortex of rats over four weeks [118] (figure 8(A)). These encouraging outcomes need to be intensively investigated in order to gain more perspective on their suitability for chronic neural implantation.

Another material is composed of stiff cellulose fibrin nanofibers encased in a soft, polymeric poly(vinyl acetate) (PVAc) matrix [122] (figure 8(B)). In the dry state, the fibers percolate with hydrogen bonds into a rigid network that confers a high elastic modulus to the system (E~4–5 GPa). Upon exposure to physiological fluids, water at 37 °C both dismantles the fiber network and reduces the PVAc glass transition to 20 °C, doubly softening the structure (E~12 MPa) [71, 119, 123] (figure 8(C)). This material demonstrated good properties in terms of mechanical tissue compliance, enhanced implantation ease and body acceptance [19]. Obviously the next step will involve study of the neural recording quality in the long run.

Globally, this line of research resembles that of hydrogels presented in the previous section. In the dry state, a hydrogel's modulus can reach higher values and so assist insertion in the cortex [32]. But as for hydrogels, the swelling of softening polymers is such (60–70% [124]) that it raises issues about material degradation, metal delamination and structural changes *in vivo* over the long term.

3.5. Bioresorbable polymers

The integration of a stiff biodegradable polymer remains the most widespread strategy for flexible probe implantation (figure 9). The polymer acts as a stiff prop during the implantation

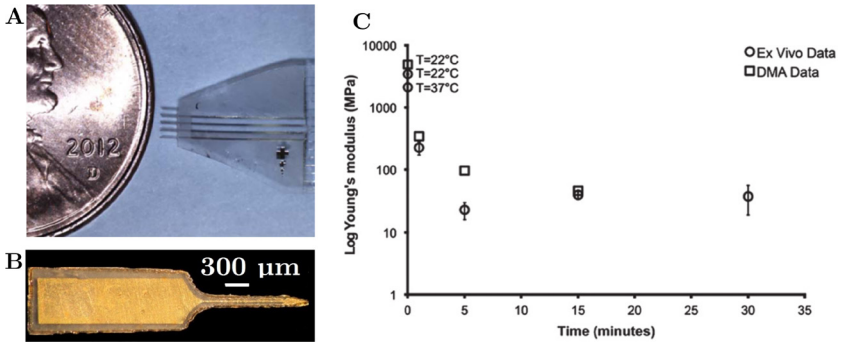

Figure 8. Mechanically-adaptive substrate. (A) Photograph of a 16-channel intracortical electrode array based on Thiol-ene acrylate substrate ([118] John Wiley & Sons. [Copyright © 2013 Wiley Periodicals, Inc].). (B) Microscope view of a laser-micromachined cortical probe made of poly(vinyl acetate) (PVAc) matrix (reproduced from [119] © IOP Publishing Ltd. All rights reserved.). (C) *In vitro* and *in vivo* drop of Young's modulus of mechanically adaptive PVAc/CNC nanocomposites as function of exposure time to ACSF or implantation time in the rat cortex (reproduced from [8] © IOP Publishing Ltd. All rights reserved.).

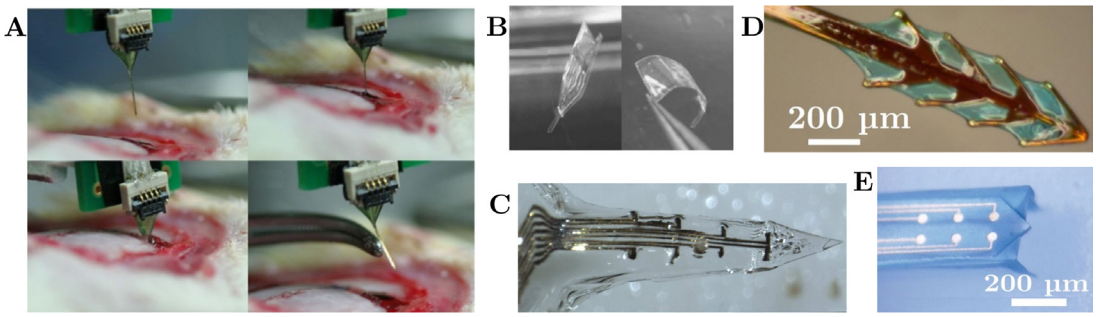

Figure 9. Example of flexible implants inserted via a bioresorbable polymer. (A) Frames of insertion *in vivo* of a maltose coated ultra-thin polyimide-based flexible neural probe (reproduced from [49] © IOP Publishing Ltd. All rights reserved.). (B) Parylene C fluidic channel filled with PEG is inserted into a gelatin tissue model (left) and recovers flexibility after insertion (right) (reproduced from [46] with permission of The Royal Society of Chemistry). (C) An electrode array before embedding into a matrix composed of gelatin, PEG and glycerol ([89] © 2015 Agorelius, Tsanakalis, Friberg, Thorbergsson, Pettersson and Schouenborg). (D) Image of a dyed silk-coated fish-bone shaped polyimide probe with tip shown (© (2011) IEEE. Reprinted, with permission, from [125]). (E) Parylene C-based neural probe back-coated with gutter-shaped dyed silk fibroin (reproduced from [41] © IOP Publishing Ltd. All rights reserved.).

procedure, providing enough stiffness to overcome the buckling force. When the probe is implanted, the polymer is in contact with physiological fluids and starts its resorption. A variety of bioresorbable polymers has been tried as candidates for enhancement of probe mechanical strength, as shown in table 1. Many materials are commercially available, such as poly(lactic-co-glycolic acid) (PLGA), polyethylene glycol (PEG), collagen/gelatin, chitosan and sucrose/maltose. Their availability provides easy access, and there is the benefit of previous knowledge regarding their use in biomedical applications. Other materials, like tyrosine-derived polycarbonate and silk, need to be synthesized, and may require some chemistry skill. The following paragraphs along with the comparison table (table 1) should help the reader understand what considerations to take into account when choosing the appropriate bioresorbable polymer for a specific application.

3.5.1. Polymer stiffness. The most obvious criterion to compare these polymers is through their stiffness. If the Young's modulus is high, the device's overall dimensions may be decreased, which leads to smaller insertion footprint and dimpling. Stiffness is also a predominant parameter when probe length is increased for deeper implantation. From this perspective, PLGA, silk, maltose/sucrose and PVAc nanocomposite might be considered more mechanically reliable for probe stiffening. For instance, silk fibroin films integrated to polyimide-based probes have shown to enable insertion of 5.5 cm long neural probes with 150 μm overall probe thickness [163]. In contrast, 300 μm diameter gelatin-coated wires were implanted only 2 mm in the cortex [139]. Typically, the bioresorbable coatings used are on the order of 80–180 μm [62, 89, 151, 163], although thinner coatings have been reported [50].

3.5.2. Dissolution and bioresorption. The fate of bioresorbable polymers involves three main steps. First, liquid uptake and temperature rise *in vivo* induces polymer swelling as well as loss of mechanical properties. Then degradation occurs, with a loss of global molecular weight due to bond breaking through enzymatic reactions [173] or hydrolysis [161]. Finally, the decomposition products are slowly removed by metabolic processes [174]. The overall resorption kinetics highly depend on water uptake capability, dimensions, crystallinity, molecular weight and hydrophilic affinity.

The loss of mechanical properties is an important drawback in the use of bioresorbable or smart polymers. The task of surgical implantation is harder, because there is a small time window for probe placement in the cortex. For instance, all fast-resorbing polymers, such as PEG [155], gelatin [142]

Table 1. Comparison table of biodegradable polymer features reported in the literature as means to stiffen a flexible neural probe.

Polymer	Young's modulus	Biocompatibility	Main biomedical applications	Degradation rate/Stiff-to-soft rate	Biochemical effect and drug integration	Sterilization
PLGA [126–128] (=PLA + PGA)	1.3–2 GPa [127, 129]	++ [129]	Resorbable sutures, bone repair, vascular graft, drug delivery [130]	Weeks to months (tunable) [127, 129, 131]	PLGA hydrogel: integrated NGF in PEG microspheres—DEX integrated in PLGA nanoparticles [126, 132]	Dry heating, autoclaving, radiation induce melting and degradation [133] Argon plasma best for PLGA sterilization [134]
Tyrosine-derived polycarbonate [135–137]	393 MPa [137]	+[138]	At research state—clinical study state for coronary stent application [137]	Hours [135]	Integrated DEX [137]	Ethylene oxide [136]
Collagen/Gelatin [28, 89, 139]	2–200 MPa (hydrated)—[140] 3.4 GPa (dehydrated) [28]	++ [141]	Artificial skin, heart valves, hemostatic agent, blood vessels prosthesis, nerve repair [141]	Minutes to hours (tunable) [142]	Haemostatic and antibacterial [139]	Autoclaving and dry heat sterilization lead to partial denaturation [143]
Chitosan [144–146]	1.2 GPa [147]	+++ [148]	Skin and bone tissue engineering, nerve and blood vessels regeneration [148]	Weeks (tunable) [149]	Haemostatic and antibacterial—integrated BNDF [148, 150]	—
Maltose/sucrose [49, 73, 151–153]	3-5 GPa [152, 154]	+[154]	Food sweetener, pharmaceutical coating [154]	Seconds to minutes [49]	—	—
PEG [46, 50, 111, 155]	0.2-2 GPa [156–158]	+++ [159]	Drug delivery, tissue regeneration [160]	Minutes [46, 111, 155]	Integrated NGF [126]-Integrated polyurethane hydrogel [161]	Ethylene oxide [111, 161]
Silk [41, 162–164]	1.7–2.8 GPa [41, 163, 165]	+++ [166, 167]	Tissue engineering (bone, cartilage, skin etc.), implant devices, suture, drug delivery [166, 167]	Seconds to weeks (tunable) [168]	Integrated NGF [169, 170]-Integrated ChABC [163]	Autoclaving, heat, ethylene oxide and ethanol show little changes in morphology, topography and crystallinity [171, 172]

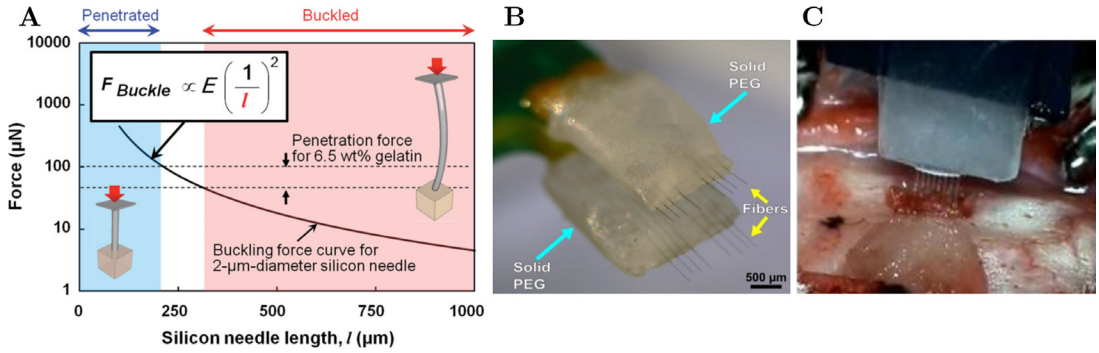

Figure 10. Reduction of effective length. (A) Buckling force versus beam length for a 2 μm-diameter silicon microneedle. Graph also includes an experimentally measured penetration force for gelatin (6.5 wt% in water). Therefore the blue region defines a regime where the needle will penetrate the brain, the red region where it would buckle on the surface ([179] John Wiley & Sons © 2015). (B) A carbon fiber array set in solidified PEG (light blue arrows) on both sides with submillimeter exposure of the fibers (yellow arrows) (reproduced from [180] © IOP Publishing Ltd. All rights reserved.). (C) The same technique has been applied to Parylene C shanks for insertion in rat hippocampus (© (2016) IEEE. Reprinted, with permission, from [181]).

and sugar-derived polymers [151], necessarily need to be implanted within minutes, and so they are not suitable for precise, fastidious implantation. Strategic integration of a fast-degrading polymer on the probe might reduce degradation kinetics: Takeuchi's team suggested a buried microchannel filled with PEG, where only the tip is in contact with body fluids [46]. In this case, diffusion limits dissolution rate. For slow-resorbing polymers, for which water affinity and crystallinity determine softening kinetics, another solution would be to adjust surface chemistry and cross-linking to improve mechanical longevity. Additionally, the drying step in processing polymers is critical, because moisture can remain in the hydrolysis-sensitive polymer, leading to accelerated degradation [174].

The degradation time, that is to say the time before all the polymer has gone through enzymatic or non-enzymatic hydrolysis, is often evaluated through *in vitro* experiments [136, 168]. Samples are immersed in PBS or a proteolytic medium at 37 °C, and collected at different times to be dried and weighed, then mass loss is calculated. However, *in vitro* studies do not take into account brain size, fluid availability and enzyme renewal, and may miscalculate the degradation time. Kozai and coworkers recently observed that bioresorbable carboxymethylcellulose coating implanted in rat brains degraded in days, when they expected complete dissolution within 20 min [175]. The authors suggest fluorescent labeling of their polymer to better track its fate in future studies.

With regard to bioresorption itself, a recurring issue affects cytotoxicity of the decomposition products and long-term side effects. The remaining low-molecular weight products of hydrolysis can interact with the surrounding cells, leading to eventual malfunction. Numerous *in vitro* and *in vivo* assays can quantify this phenomenon before clinical trials [176]. It has been noted that bio-derived polymers such as collagen and chitosan tend to induce less inflammatory response linked to degradation compounds than synthesized polymers [174].

3.5.3. Biocompatibility and sterilization. As mentioned earlier, commercially available polymers have generally more information available as to their biocompatibility, for many have been used for decades in other biomedical applications, including tissue engineering, drug delivery and grafts [130, 141]. Chitosan and collagen both present with intrinsic haemostatic and antibacterial properties, which help soothe foreign body responses [141, 148]. However, clinical observations have shown indications that about 3% of the total population would present with an inherent immunity (allergy) to bovine-type collagen [177].

Sterilization also plays a part in device biocompatibility. Sterilization must be performed after fabrication to reduce the risk of infections and possible complications. It can be achieved either through chemical means (ethanol 70%), dry heating (160–190 °C), autoclaving (120–135 °C), ethylene oxide gas or UV radiation, in agreement with biomedical device regulation [178]. However, several common sterilization methods are not compatible with numerous biodegradable polymers, primarily due to their low thermal stability and hydrolytic degradation mechanisms [133, 172]. The sterilization methods that were used are listed on table 1.

3.6. Reduction of effective length

At this point, it is important to stress that probe length plays a major role in device mechanical failure. As seen in equation (1), the buckling force is proportional to $\frac{1}{L^2}$, and a slight increase in length results in a substantial drop in a probe's stiffness. For this reason, the targeted brain area is a predominant factor in the choice of a stiffening strategy. As a way to insert long penetrating shanks into the brain, the stiffening structure can also be integrated as a base scaffold for the probes. One can adjust the scaffold length l so that the probe buckling force, which is proportional to $\frac{1}{(L-l)^2}$, can be greater than the insertion force (figure 10(A)). In a recent study, arrays of high aspect ratio microneedles were shown to withstand deep implantation when coupled with a silk base structure that temporarily reduces device length [179]. This bioresorbable structure is then dissolved in saline in order to insert the devices over their whole length. This technique has found interest in the insertion of arrays (2D) and matrices (3D) of

shanks, because it uses only one manipulation to stiffen all the probes at once [180, 181], when the integration of one coating per probe might be particularly burdensome (figures 10(B) and (C)).

4. Discussion and engineered solutions

4.1. Insertion conditions and footprint

The insertion mechanisms of traditional, silicon-based single neural probe or tungsten wires have been the subject of many studies [101–104]. The mechanical trauma of insertion leads to vessel rupture, tissue dimpling and compression, and neuron severing [182] (figure 11).

Studies have assessed the influence of many insertion parameters such as tip geometry, insertion speed and probe diameter [11, 105, 106]. It is generally admitted that a fine tip decreases tissue dimpling and vessel dragging [11, 183], and that probe dimension plays a major role in the reduction of shear force and inflammatory response [21, 87, 128]. However, insertion speed does not benefit from such consensus, as seen in table 2. On the one hand, a fast insertion is meant to compensate for poor tip design, and will transect membranes and vessels instead of dragging them. On the other hand a slow insertion will allow for tissue relaxation and accommodation of compression forces with minimal shock [105, 183].

Moreover, there is no essential consensus over the importance of initial insertion footprint. Szarowski *et al* pointed out that if the early response (<1 week) seemed proportional to device cross-section, the sustained response was similar for a wide range of device geometries [186]. Two other studies pointed out a concrete relationship between implant width and inflammation at four weeks [128] and at 12 weeks [87] post-implantation. These findings confirm the link between compliance and inflammation soothing over time, but there is no direct link between the initial insertion footprint and the sustained glial response. The closing of brain tissue around the implant once an insertion shuttle is removed or once a polymer coating is resorbed is not clearly described in the literature, and one could assume that the footprint is of little importance if the final design is thin and compliant. This timing issue can be all the more preponderant in the case of resorbable polymers that depend on the dissolution and degradation time, volume increase due to swelling might extend the injury beyond the initial footprint.

Besides these theoretical considerations, implant type (single shank or 3D arrays) and material (silicon or soft polymer), insertion depth (surface or deep) and procedure (animal type, age or brain region targeted) or setup (manual or pneumatic insertion tool) might not leave room for much choice. For instance, thin, compliant, or flexible probes cannot be inserted at high speed because they are fragile and will buckle or break when the insertion is too fast [97]. Most studies focused on the insertion of a silicon shank or tungsten wire, and the lack of knowledge concerning the mechanical insertion of flexible neural probes is regrettable.

Implantation mechanisms can sever the device regardless of its nature. A study by Ward and coworkers showed

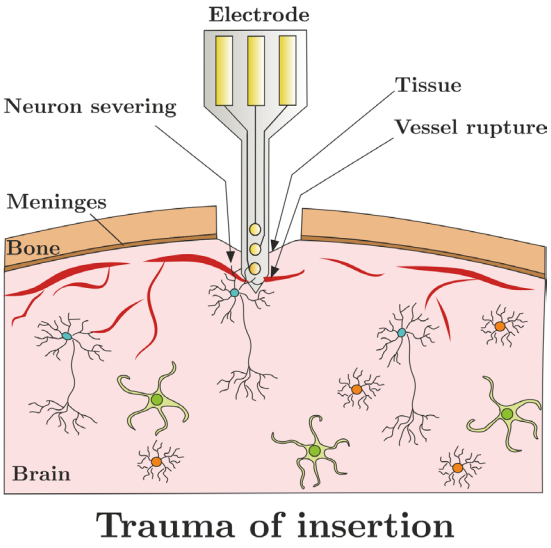

Figure 11. Schematic representation of the trauma of insertion involved in the implantation of a chronic probe in the brain. During surgical implantation, the probe induces dimpling of the brain surface before actual insertion, and severs capillaries and neurons as it makes its path.

that seven of nineteen commercially-available intracortical devices suffered from mechanical failure upon insertion [187]. Microshanks made of brittle silicon can break upon insertion in the cortex, glass pipette tips are also quite fragile, and flexible microprobes can experience compression forces that might generate connectic breakage or faulty contact. More generally, surgical handling of small, fragile devices with unreliable packaging leads to a certain percentage of electrode failure after surgical implantation [10, 188].

4.2. Bioactive tissue interface

One of the greatest advantages of the coatings technologies discussed (bioresorbable polymers, hydrogels) is that they are able to soothe foreign body reactions, through biochemical features or the incorporation of bioactive agents. Cellular attachment active substances, anti-inflammatory agents and neurotrophins, as well as embedding of neural cells, are investigated as alternatives towards body acceptance. For a more comprehensive understanding of the subject, we direct the reader towards reviews focusing on the biochemical features of organic device coatings rather than the mechanical features [4, 32, 189].

Bioactive agents. Drugs can be blended within polymer coatings through non-covalent binding, such as adsorption, physical entrapment or electrostatic interactions, and covalent binding [189] (figure 12(A)).

For bioresorbable polymers, release kinetics are usually hard to quantify, because a number of parameters needs to be taken into account. The time during which the drug is released at functional levels from the host polymer depends on binding strength, host degradation rate and diffusion mechanisms, among others. For this reason, only a percentage of the total amount of drug implanted is actually bioactive. For instance, silk fibroin co-dissolved with nerve growth factor (NGF)

Table 2. Non-exhaustive comparison table of *in vitro* or *in vivo* neural probe insertion parameters studied in the literature.

	Insertion speeds used in the study (in μm s^{-1})		Device material	Design	Cross-section (μm)	Tip angle (°)	Insertion depth (mm)
	Min	Max					
Rennaker *et al* [184]	1.5–3.5	1.5×10^6	Tungsten wire	2×7 array (250 μm pitch)	$\emptyset$50	unknown	0.6/3
Tian *et al* [101]	50	400	Tungsten wire	Single shaft or 3×3 array (pitch 500 μm)	$\emptyset$50	unknown	$\geqslant 3$
Bjornsson *et al* [11]	125	2000	Silicon	Single shaft	60×100	5–150	< 2
Hosseini *et al* [100]	~85–160	~1670	Silicon	Single shaft or 1×10 array (pitch 550/1100 μm)	100×120	17	3–6
			Glass	Single shaft	175×500	49.3	
			Polyimide		10×460	66	
			Tungsten		$\emptyset$135	15–20	
Andrei and Welkenhuysen *et al* [105, 106]	10	100	Silicon	Single shaft	[200–400] $\times$[50 − 150]	10–50	6
Fekete *et al* [185]	20	175	Silicon	Single shaft	[200–400] $\times$400	0–90	~2–3

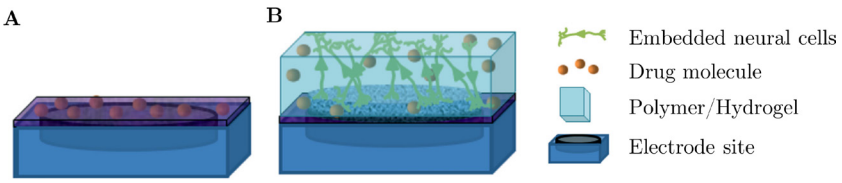

Figure 12. Schematic illustrations of electrode site coated with (A) biologically active molecules and (B) neural cells embedded in a hydrogel matrix (reproduced with permission from [32]).

lowered the availability of the protein to a concentration of 50–70% of the actual amount (180 ng mg^{-1}) [170]. Brain-derived neurotrophic factor (BDNF) can be blended with chitosan scaffolds using genepin as a cross-linking agent [150]. Nerve Growth Factor (NGF), another regeneration-enhancing agent, can be integrated in PEG microspheres in a PLGA matrix, where PEG acts as a porogen to control the release rate of NGF [190]. This same drug was also blended with silk fibroin, forming nerve conduits that successfully released bioactive NGF over four weeks and promoted PC12 cell differentiation with neurite outgrowth [170]. Silk fibroin mixed with chondroitinase ABC (ChABC) was reported to be functional *in vitro* [163]. On the other hand, the ability of dexamethasone (DEX)-blended tyrosine-derived terpolymer to locally deliver this anti-inflammatory drug was shown *in vitro*, but the *in vivo* study showed no qualitative difference between the tissue reactions to coated and uncoated wires [137]. Anti-oxydant curcumin-releasing softening polymer implants presented with higher neuron survival and a more stable blood–brain barrier than without curcumin at four weeks post-implantation, yet showed no biological improvements at 12 weeks [191].

The combination of numerous bioactive agents has proven effective for the reduction of inflammation, and its combination with compliance approaches might lead to minimally-scarring devices. In a recent study, Parylene C sheath electrodes were coated with Matrigel containing a cocktail of bioactive agents (DEX, BDNF and NGF) as well as a virally-mediated expression of Caveolin-1, and implanted in rat brains over 12 months. Their results indicate a strong relation between the rise in the neural signaling and histologically observable dendritic sprouting, which supports the importance of creating a bio-friendly environment around the neural probes through different means (flexible implant, bioactive agents).

Cellular modifications. Another emerging approach from the tissue engineering literature is the integration of neural cells within a polymer coating. This method is based on the assumption that neural tissue should grow more effectively on a brain cell-mimicking layer on the electrode surface, creating an intimate junction between device and target [192]. A study by Richter *et al* integrated pancreatic stem cells seeded over a polyimide surface. A fibrin hydrogel protected these cells from the mechanical insertion shear forces, and overall should significantly enhance device acceptance [193]. Purcell *et al* also seeded an open well with neural stem cells encapsulated in an alginate hydrogel scaffold over a Parylene neuroprosthesis, and their structure resulted in an attenuation of the initial tissue response [194].

According to Aregueta-Robles *et al* the ideal tissue engineered interface should incorporate combined coating approaches of conductive polymers, hydrogels and attachment factors with neural cells (figure 12(B)).

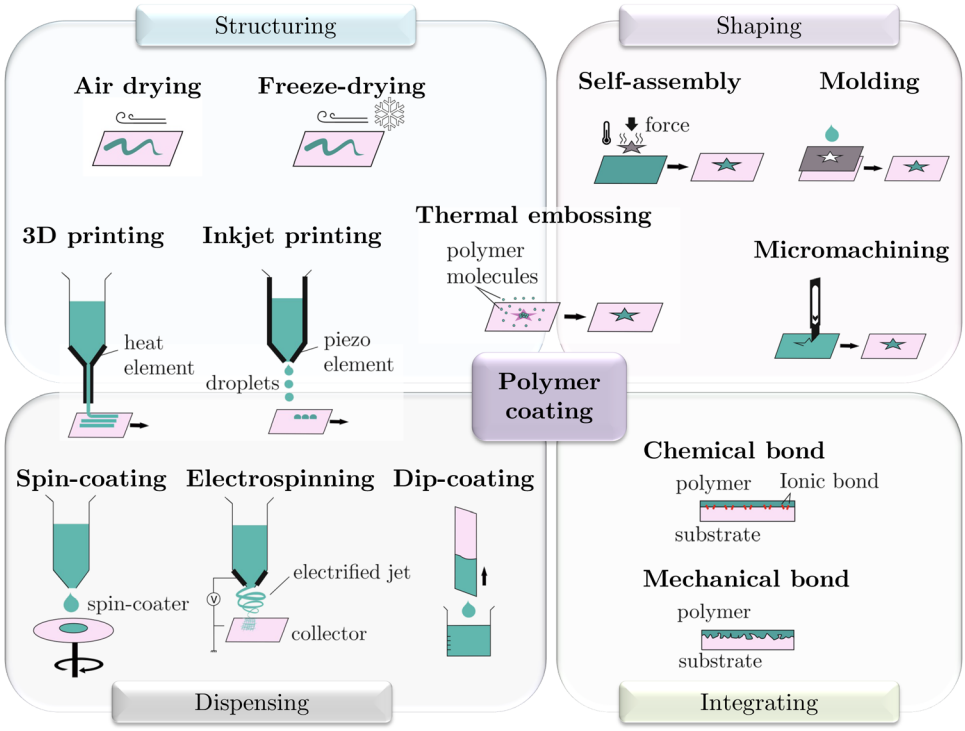

Figure 13. Methods to obtain a polymer coating on a substrate in relation to the considerations to be taken into account: how to get the polymer onto the substrate (dispensing), how to outline the structure (shaping), what kind of crystalline structure is needed (structuring) and how it will adhere to the substrate (integrating). Non-exhaustive examples of the four considerations are displayed, referenced from the literature in tissue engineering.

4.3. Coating formation

The mechanical and surface properties of a neural probe with an engineered polymeric surface is highly dependent on how it is obtained. The most commonly reported way to integrate a polymer or hydrogel onto a flexible probe is dip-coating, where the device is immersed in a diluted polymer [21, 23, 29, 49, 125, 151]. Thickness control is defined by the immersion and retraction speed, the solution concentration, and the number of coatings. However, this method implies that both sides of the device are covered with polymer, which might act as an insulating layer that would compromise electrical recording, though hydrogels are generally poor insulators due to the swollen mesh structure in physiological fluids [32]. An acrylic or elastomer mold might prove useful for structuring and shaping the polymer to certain dimensions and form factors [28, 41, 71, 155, 163, 195]. Another solution is to fill a closed or open channel inside the probe with a desired bioresorbable polymer [46, 196].

It is worth noting that the scope of methods used in the literature is narrow compared to the various reported methods for obtaining a polymer coating with controlled shape and structure. Indeed, research in tissue engineering has furthered and widened the field in terms of dispensing, shaping, structuring and integrating polymers [197] (figure 13).

While dip-coating, spin-casting and inkjet printing have been used for decades as dispensing techniques in other fields, the use of 3D printing and electrospinning has recently developed as part of the tissue engineering process. Electrospinning natural or synthesized biomaterials has the advantage of forming a biomimetic microstructure resembling the extracellular matrix. Electrospun PLLA and silk nanofibrous scaffolds have for instance gained considerable interest in peripheral nerve repair [198–200]. With emerging techniques and increasing applications, 3D printing has become quite the fashionable additive manufacturing method over the past few years. Particularly, chitosan and PLA-based 3D-printed scaffolds have already shown interesting possibilities for tissue engineering [201]. Unfortunately, the resolution for 3D-printed biomaterials is still in the order of hundreds of microns depending on the technique used [202], which restrains broadcast use for microsystems. Finally, inkjet printing methods can reach smaller dimensions for either dispensing the polymer itself (e.g. silk [203]) or a cross-linking agent or solvent for the already cast polymer [204].

Whenever the dispensing technique does not involve dimension control, shaping the polymer layer is essential to match the implant size. As mentioned before, casting and molding is the simplest way to obtain a polymer of desired shape. However, other methods such as micromachining through laser cutting techniques, mechanical carving or plasma etching can be applied, depending on the material and the resolution needed. Also, a thin layer can be formed onto the probe surface through self-assembling of complementary peptides in aqueous solutions [197].

In other cases, surface properties may not promote coating integration, but still play a great role in the adhesion between the polymer and its substrate. For water-based polymers, a hydrophilic neural probe will enhance the bond with

its coating [41], and surface roughness or an intermediate layer might prove useful to obtain a strong mechanical bond between the two layers.

Finally the overall structure, roughness, porosity and surface chemistry of the polymer coating can be altered using a different solvent or solvent evaporation method. Unfortunately, most dispensing and structuring techniques do not allow for a varied solvent option. Freeze-drying tends to form more porous materials, such as chitosan, helpful for bioactive agent integration but eventually reducing the stiffness [205]. On the other hand, thermal embossing of PLGA has been shown to avoid the use of potentially dangerous solvents such as chloroform [127].

5. Conclusion

Reliability and stability of chronic intracortical recording or stimulation bring out many issues yet to be addressed. Among them, device acceptability and material lifetime are strongly correlated to inconsistent recordings and premature failure. The reduction of mechanical mismatch can be achieved via a variety of means, including matching the Young's modulus, implant geometry, fixation mode and the addition of a hydrogel coating. These strategies are based on the assumption that a better mechanical compliance with the surrounding tissues leads to greater signal stability.

Insertion mechanisms remain poorly understood, and smaller, flexible devices tend to fail during surgical implantation. Indeed, depending on shank length, probe material and dimension, the new generation of chronic implants can barely withstand insertion forces. The smallest change in brain tissue hardness, linked to anatomic anisotropy, age and species considered, will most likely cause the device to fail during the penetration stage.

A wide number of strategies have arisen to confer mechanical support and compliance for the electrodes. Many of them promote the addition of a polymer coating to the probe that either improve the electrode interface and/or will assist insertion. The impact of such methods goes beyond simple mechanical assistance, as the polymer acts as a biofriendly coating that soothes the foreign body response. The choice of polymer type and its integration must be made carefully keeping the application in mind, as a variety of parameters depends on it, such as stiffness, degradation rate, bioresorbability and bioactive capability. Smart polymers, such as thermo and chemoresponsive polymers, have also shown great promise for such applications.

For some time the techniques used have been highly application-dependent and have been implemented to address a specific target. Opportunities to develop complex structures, with controlled shape, dimension, morphology and degradability have only started to be seized. Increased inspiration from tissue engineering research would help design polymer-based, highly tunable cortical devices that are able to not only overcome mechanical issues, but also enhance chronic stability through biochemical means.

Ultimately, one challenge of the decade is to design reliable 2D and 3D arrays of compliant probes with numerous recording sites, that could be used in high-resolution BCIs. This scaling-up will inevitably bring out other issues with insertion mechanisms. Indeed, inserting several dozens of shanks with minimal dimpling and insertion footprint will be the most challenging.

Acknowledgments

The authors would like to thank Pr Jed Harrison from the University of Alberta and Dr Laurent Malaquin from the LAAS laboratory for their inputs on this work. Part of this work was financed by ANR Neuromeddle 15-CE19-0006. The PhD grant of A Lecomte was allocated by CNRS-INSIS.

References

[1] Donoghue J P 2008 Bridging the brain to the world: a perspective on neural interface systems *Neuron* **60** 511–21
[2] Birbaumer N 2006 Breaking the silence: brain-computer interfaces (BCI) for communication and motor control *Psychophysiology* **43** 517–32
[3] Brumberg J S, Nieto-Castanon A, Kennedy P R and Guenther F H 2010 Brain-computer interfaces for speech communication *Speech Commun.* **52** 367–79
[4] Fattahi P, Yang G, Kim G and Abidian M R 2015 A review of organic and inorganic biomaterials for neural interfaces *Adv. Mater.* **26** 1846–85
[5] Carmena J M, Lebedev M, Crist R E, O'Doherty J E, Santucci D M, Dimitrov D F, Patil P G, Henriquez C S and Nicolelis M L 2003 Learning to control a brain-machine interface for reaching and grasping by primates *PLoS Biol.* **1** 193–208
[6] Collinger J L, Wodlinger B, Downey J E, Wang W, Tyler-Kabara E C, Weber D J, McMorland A J C, Velliste M, Boninger M L and Schwartz A B 2013 High-performance neuroprosthetic control by an individual with tetraplegia *Lancet* **381** 557–64
[7] Cogan S F 2008 Neural stimulation and recording electrodes *IEEE Eng. Med. Biol. Soc.* **10** 275–309
[8] Jorfi M, Skousen J L, Weder C and Capadona J R 2015 Progress towards biocompatible intracortical microelectrodes for neural interfacing applications *J. Neural Eng.* **12** 011001
[9] Nolta N F, Christensen M B, Crane P D, Skousen J L and Tresco P A 2015 BBB leakage, astrogliosis, and tissue loss correlate with silicon microelectrode array recording performance *Biomaterials* **53** 753–62
[10] Prasad A, Xue Q-S, Sankar V, Nishida T, Shaw G, Streit W J and Sanchez J C 2012 Comprehensive characterization and failure modes of tungsten microwire arrays in chronic neural implants *J. Neural Eng.* **9** 056015
[11] Bjornsson C S, Oh S J, Al-Kofahi Y, Lim Y J, Smith K L, Turner J N, De S, Roysam B, Shain W and Kim S J 2006 Effects of insertion conditions on tissue strain and vascular damage during neuroprosthetic device insertion *J. Neural Eng.* **3** 196–207
[12] Aimedieu P and Grebe R 2004 Tensile strength of cranial pia mater: preliminary results *J. Neurosurgery* **100** 111–4
[13] Muthuswamy J, Saha R and Gilletti A 2005 Tissue micromotion induced stress around brain implants *3rd IEEE/EMBS Special Topic Conf. on Microtechnology in Medicine and Biology* vol 2005 pp 102–3
[14] Subbaroyan J, Martin D C and Kipke D R 2005 A finite-element model of the mechanical effects of implantable

microelectrodes in the cerebral cortex *J. Neural Eng.* **2** 103–13
[15] Sridharan A, Nguyen J K, Capadona J R and Muthuswamy J 2015 Compliant intracortical implants reduce strains and strain rates in brain tissue *in vivo J. Neural Eng.* **12** 036002
[16] Sridharan A, Rajan S D and Muthuswamy J 2013 Long-term changes in the material properties of brain tissue at the implant-tissue interface *J. Neural Eng.* **10** 066001
[17] Polanco M, Bawab S and Yoon H 2016 Computational assessment of neural probe and brain tissue interface under transient motion *Biosensors* **6** 1–13
[18] Polikov V S, Tresco P A and Reichert W M 2005 Response of brain tissue to chronically implanted neural electrodes *J. Neurosci. Methods* **148** 1–18
[19] Nguyen J K, Park D J, Skousen J L, Hess-Dunning A E, Tyler D J, Rowan S J, Weder C and Capadona J R 2014 Mechanically-compliant intracortical implants reduce the neuroinflammatory response *J. Neural Eng.* **11** 056014
[20] Kozai T D Y, Jaquins-Gerstl A S, Vazquez A L, Michael A C and Cui X T 2015 Brain tissue responses to neural implants impact signal sensitivity and intervention strategies *ACS Chem. Neurosci.* **6** 48–67
[21] Skousen J L, Bridge M J and Tresco P A 2015 A strategy to passively reduce neuroinflammation surrounding devices implanted chronically in brain tissue by manipulating device surface permeability *Biomaterials* **36** 33–43
[22] Green R A, Hassarati R T, Goding J A, Baek S, Lovell N H, Martens P J and Poole-Warren L A 2012 Conductive hydrogels: mechanically robust hybrids for use as biomaterials *Macromol. Biosci.* **12** 494–501
[23] Abidian M R and Martin D C 2009 Multifunctional nanobiomaterials for neural interfaces *Adv. Funct. Mater.* **19** 573–85
[24] Fekete Z 2015 Recent advances in silicon-based neural microelectrodes and microsystems *Sensors Actuators* B **215** 300–15
[25] Wise K D 2005 Silicon microsystems for neuroscience and neural prostheses *IEEE Eng. Med. Biol. Mag.* **24** 22–9
[26] Ruther P, Herwik S, Kisban S, Seidl K and Paul O 2010 Recent progress in neural probes using silicon MEMS technology *IEEJ Trans. Electr. Electron. Eng.* **5** 505–15
[27] Ahmed T A E, Dare E V and Hincke M 2008 Fibrin: a versatile scaffold for tissue engineering applications *Tissue Eng.* B **14** 199–215
[28] Shen W, Karumbaiah L, Liu X, Saxena T, Chen S, Patkar R, Bellamkonda R V and Allen M G 2015 Extracellular matrix-based intracortical microelectrodes: Toward a microfabricated neural interface based on natural materials *Microsyst. Nanoeng.* **1** 15010
[29] Abidian M R, Daneshvar E D, Egeland B M, Kipke D R, Cederna P S and Urbanchek M G 2012 Hybrid conducting polymer-hydrogel conduits for axonal growth and neural tissue engineering *Adv. Healthcare Mater.* **1** 762–7
[30] Mario Cheong G L, Lim K S, Jakubowicz A, Martens P J, Poole-Warren L A and Green R A 2014 Conductive hydrogels with tailored bioactivity for implantable electrode coatings *Acta Biomater.* **10** 1216–26
[31] Zieris A, Prokoph S, Levental K R, Welzel P B, Chwalek K, Schneider K, Freudenberg U and Werner C 2012 Sustainable frowth factor delivery through affinity-based adsorption to starPEG-Heparin hydrogels *Proteins at Interfaces III State of the Art (ACS Symp. Series* vol 1120) ed T Horbett *et al* ch 24, pp 525–41
[32] Aregueta-Robles U A, Woolley A J, Poole-Warren L A, Lovell N H and Green R A 2014 Organic electrode coatings for next-generation neural interfaces *Front. Neuroeng.* **7** 15
[33] Green R A, Suaning G J, Poole-Warren L A and Lovell N H 2009 Bioactive conducting polymers for neural interfaces: application to vision prosthesis *4th Int. IEEE/EMBS Conf. on Neural Engineering* pp 60–3
[34] Green R and Abidian M R 2015 Conducting polymers for neural prosthetic and neural interface applications *Adv. Mater.* **27** 7620–37
[35] Abidian M R, Corey J M, Kipke D R and Martin D C 2010 Conducting-polymer nanotubes improve electrical properties, mechanical adhesion, neural attachment, and neurite outgrowth of neural electrodes *Small* **6** 421–9
[36] Ates M 2013 A review study of (bio)sensor systems based on conducting polymers *Mater. Sci. Eng.* C **33** 1853–9
[37] Abidian M R, Salas L G, Yazdan-Shahmorad A, Marzullo T C, Martin D C and Kipke D R 2007 *In vivo* evaluation of chronically implanted neural microelectrode arrays modified with poly (3,4-ethylenedioxythiophene) nanotubes *Proc. of the 3rd Int. IEEE EMBS Conf. on Neural Engineering* pp 61–4
[38] Kim D H, Wiler J A, Anderson D J, Kipke D R and Martin D C 2010 Conducting polymers on hydrogel-coated neural electrode provide sensitive neural recordings in auditory cortex *Acta Biomater.* **6** 57–62
[39] Lee K Y, Rowley J A, Eiselt P, Moy E M, Bouhadir K H and Mooney D J 2000 Controlling mechanical and swelling properties of alginate hydrogels independently by cross-linker type and cross-linking density *Macromolecules* 4291–4
[40] Guiseppi-Elie A 2010 Electroconductive hydrogels: Synthesis, characterization and biomedical applications *Biomaterials* **31** 2701–16
[41] Lecomte A, Castagnola V, Descamps E, Dahan L, Blatché M, Leclerc E and Bergaud C 2015 Silk and PEG as means to stiffen a parylene probe for insertion in the brain: toward a double time-scale tool for local drug delivery *J. Micromech. Microeng.* **25** 125003
[42] Altuna A *et al* 2013 SU-8 based microprobes for simultaneous neural depth recording and drug delivery in the brain *Lab Chip* **13** 1422–30
[43] Mercanzini A, Cheung K, Buhl D L, Boers M, Maillard A, Colin P, Bensadoun J-C, Bertsch A and Renaud P 2008 Demonstration of cortical recording using novel flexible polymer neural probes *Sensors Actuators* A **143** 90–6
[44] Ware T, Simon D, Rennaker R L and Voit W 2013 Smart polymers for neural interfaces *Polymer Rev.* **53** 108–29
[45] Moshayedi P, Ng G, Kwok J C F, Yeo G S H, Bryant C E, Fawcett J W, Franze K and Guck J 2014 The relationship between glial cell mechanosensitivity and foreign body reactions in the central nervous system *Biomaterials* **35** 3919–25
[46] Takeuchi S, Ziegler D, Yoshida Y, Mabuchi K and Suzuki T 2005 Parylene flexible neural probes integrated with microfluidic channels *Lab Chip* **5** 519–23
[47] Huang S H, Lin S P and Chen J J J 2014 *In vitro* and *in vivo* characterization of SU-8 flexible neuroprobe: from mechanical properties to electrophysiological recording *Sensors Actuators* A **216** 257–65
[48] Fekete Z and Pongrácz A 2017 Multifunctional soft implants to monitor and control neural activity in the central and peripheral nervous system: a review *Sensors Actuators* B **243** 1214–23
[49] Xiang Z, Yen S-C, Xue N, Sun T, Tsang W M, Zhang S, Liao L-D, Thakor N V and Lee C 2014 Ultra-thin flexible polyimide neural probe embedded in a dissolvable maltose-coated microneedle *J. Micromech. Microeng.* **24** 065015
[50] Chen C-H, Chuang S-C, Su H-C, Hsu W-L, Yew T-R, Chang Y-C, Yeh S-R and Yao D-J 2011 A three-dimensional flexible microprobe array for neural recording assembled through electrostatic actuation *Lab Chip* **11** 1647–55
[51] Castagnola V, Descamps E, Lecestre A, Dahan L, Remaud J, Nowak L and Bergaud C 2014 Parylene-based flexible

neural probes with PEDOT coated surface for brain stimulation and recording *Biosensors and Bioelectronics* vol 67 (Amsterdam: Elsevier) pp 450–7
[52] Weltman A, Yoo J and Meng E 2016 Flexible, penetrating brain probes enabled by advances in polymer microfabrication *Micromachines* **7** 180
[53] Kim B J, Kuo J T W, Hara S A, Lee C D, Yu L, Gutierrez C A, Hoang T Q, Pikov V and Meng E 2013 3D Parylene sheath neural probe for chronic recordings *J. Neural Eng.* **10** 45002
[54] Kuo J T W, Kim B J, Hara S A, Lee C D, Gutierrez C A, Hoang T Q and Meng E 2013 Novel flexible Parylene neural probe with 3D sheath structure for enhancing tissue integration *Lab Chip* **13** 554–61
[55] Metallo C, White R D and Trimmer B A 2011 Flexible parylene-based microelectrode arrays for high resolution EMG recordings in freely moving small animals *J. Neurosci. Methods* **195** 176–84
[56] Hassler C, von Metzen R P, Ruther P and Stieglitz T 2010 Characterization of Parylene C as an encapsulation material for implanted neural prostheses *J. Biomed. Mater. Res.* B **93** 266–74
[57] Seymour J P, Elkasabi Y M, Chen H Y, Lahann J and Kipke D R 2009 The insulation performance of reactive parylene films in implantable electronic devices *Biomaterials* **30** 6158–67
[58] Minnikanti S, Diao G, Pancrazio J J, Xie X, Rieth L, Solzbacher F and Peixoto N 2014 Lifetime assessment of atomic-layer-deposited Al2O3-Parylene C bilayer coating for neural interfaces using accelerated age testing and electrochemical characterization *Acta Biomater.* **10** 960–7
[59] Lo H W and Tai Y C 2007 Characterization of parylene as a water barrier via buried-in pentacene moisture sensors for soaking tests *Int. Conf. on Nano/Micro Engineered and Molecular Systems* pp 872–5
[60] Lee C D, Hara S A, Yu L, Kuo J T W, Kim B J, Hoang T, Pikov V and Meng E 2015 Matrigel coatings for Parylene sheath neural probes *J. Biomed. Mater. Res.* B **104** 357–68
[61] Hara S A, Kim B J, Kuo J T W, Lee C D, Meng E and Pikov V 2016 Long-term stability of intracortical recordings using perforated and arrayed Parylene sheath electrodes *J. Neural Eng.* **13** 066020
[62] Lecomte A, Degache A, Descamps E, Dahan L and Bergaud C 2017 *In vitro* and *in vivo* biostability assessment of chronically-implanted Parylene C neural sensors *Sensors Actuators* B 251 1001–8
[63] Lee K-K, He J, Singh A, Massia S, Ehteshami G, Kim B and Raupp G 2004 Polyimide-based intracortical neural implant with improved structural stiffness *J. Micromech. Microeng.* **14** 32–7
[64] Murray S, Hillman C and Pecht M 2004 Environmental aging and deadhesion of polyimide dielectric films *J. Electron. Packag.* **126** 390
[65] Stieglitz T, Beutel H, Schuettler M and Meyer J-U 2000 Micromachined, polyimide-based devices for flexible neural interfaces *Biomed. Microdevices* **2** 283–94
[66] Rubehn B and Stieglitz T 2010 *In vitro* evaluation of the long-term stability of polyimide as a material for neural implants *Biomaterials* **31** 3449–58
[67] Lago N, Yoshida K, Koch K P and Navarro X 2007 Assessment of biocompatibility of chronically implanted polyimide and platinum intrafascicular electrodes *IEEE Trans. Biomed. Eng.* **54** 281–90
[68] Altuna A, Gabriel G, Menéndez de la Prida L, Tijero M, Guimerá A, Berganzo J, Salido R, Villa R and Fernández L J 2010 SU-8-based microneedles for *in vitro* neural applications *J. Micromech. Microeng.* **20** 064014
[69] Rubehn B, Wolff S B E, Tovote P, Lüthi A and Stieglitz T 2013 A polymer-based neural microimplant for optogenetic applications: design and first *in vivo* study *Lab Chip* **13** 579–88
[70] Lee B, Jin J, Park J and Kim J 2013 Flexible neural probe integrated microchannel and optical fiber for multiple stimulation *17th Int. Solid-State Sensors, Actuators and Microsystems Conf., Transducers (Barcelona, Spain, 16–20 June 2013)* pp 321–4
[71] Harris J P, Hess A E, Rowan S J, Weder C, Zorman C A, Tyler D J and Capadona J R 2011 *In vivo* deployment of mechanically adaptive nanocomposites for intracortical microelectrodes *J. Neural Eng.* **8** 046010
[72] Lee S E, Jun S B, Lee H J, Kim J, Lee S W, Im C, Shin H C, Chang J W and Kim S J 2012 A flexible depth probe using liquid crystal polymer *IEEE Trans. on Biomedical Engineering* pp 2085–94
[73] Singh A, Zhu H and He J 2004 Improving mechanical stiffness of coated benzocyclobutene (BCB) based neural implant *IEEE Eng. Med. Biol. Soc.* **6** 4298–301
[74] David-Pur M, Bareket-Keren L, Beit-Yaakov G, Raz-Prag D and Hanein Y 2014 All-carbon-nanotube flexible multi-electrode array for neuronal recording and stimulation *Biomed. Microdevices* **16** 43–53
[75] Minev I R *et al* 2015 Electronic dura mater for long-term multimodal neural interfaces *Science* **347** 159–63
[76] Lee J N, Jiang X, Ryan D and Whitesides G M 2004 Compatibility of mammalian cells on surfaces of poly(dimethylsiloxane) *Langmuir* **20** 11684–91
[77] Lind G, Linsmeier C E and Schouenborg J 2013 The density difference between tissue and neural probes is a key factor for glial scarring *Nat. Sci. Rep.* **3** 2942
[78] Von Metzen R P and Stieglitz T 2013 The effects of annealing on mechanical, chemical, and physical properties and structural stability of Parylene C *Biomed. Microdevices* **15** 727–35
[79] Hsu J-M, Rieth L, Kammer S, Orthner M and Solzbacher F 2008 Effect of thermal and deposition processes on the surface morphology, crystallinity, and Adhesion of Parylene-C *Sens. Mater* **20** 87–102
[80] Chang J H C, Lu B and Tai Y C 2011 Adhesion-enhancing surface treatments for parylene deposition *16th Int. Solid-State Sensors, Actuators and Microsystems Conf., 16th Int. Solid-State Sensors, Actuators and Microsystems Conf.,Transducers (Beijing, China, 5–9 June 2011)* pp 390–3
[81] Xie X, Rieth L, Caldwell R, Diwekar M, Tathireddy P, Sharma R and Solzbacher F 2013 Long-term bilayer encapsulation performance of atomic layer deposited Al2O3 and Parylene C for biomedical implantable devices *IEEE Trans. Biomed. Eng.* **60** 2943–51
[82] Hogg A, Uhl S, Feuvrier F, Girardet Y, Graf B, Aellen T, Keppner H, Tardy Y and Burger J 2014 Protective multilayer packaging for long-term implantable medical devices *Surf. Coat. Technol.* **255** 124–9
[83] Pei W *et al* 2014 Silicon-based wire electrode array for neural interfaces *J. Micromech. Microeng.* **24** 095015
[84] Najafi K, Ji J and Wise K D 1990 Scaling limitations of silicon multichannel recording probes *IEEE Trans. Biomed. Eng.* **37** 1–11
[85] Bezzina C, Verret L, Juan C, Remaud J, Halley H, Rampon C and Dahan L 2015 Early onset of hypersynchronous network activity and expression of a marker of chronic seizures in the Tg2576 mouse model of Alzheimer's disease *PLoS One* **10** 1–14
[86] Benabid A L 2003 Deep brain stimulation for Parkinson disease *Curr. Opin. Neurobiol.* **13** 696–706
[87] Thelin J, Jörntell H, Psouni E, Garwicz M, Schouenborg J, Danielsen N and Linsmeier C E 2011 Implant size and fixation mode strongly influence tissue reactions in the CNS *PLoS One* **6** e16267

[88] Sankar V, Sanchez J C, McCumiskey E, Brown N, Taylor C R, Ehlert G J, Sodano H A and Nishida T 2013 A highly compliant serpentine shaped polyimide interconnect for front-end strain relief in chronic neural implants *Front. Neurol.* **4** 124

[89] Agorelius J, Tsanakalis F, Friberg A, Thorbergsson P T, Pettersson L M E and Schouenborg J 2015 An array of highly flexible electrodes with a tailored configuration locked by gelatin during implantation: initial evaluation in cortex cerebri of awake rats *Front. Neurosci.* **9** 1–12

[90] Huang R, Pang C, Tai Y C, Emken J, Ustun C, Andersen R and Burdick J 2008 Integrated parylene-cabled silicon probes for neural prosthetics *IEEE MEMS* pp 240–3

[91] Sommakia S, Lee H C, Gaire J and Otto K J 2014 Materials approaches for modulating neural tissue responses to implanted microelectrodes through mechanical and biochemical means *Curr. Opin. Solid State Mater. Sci.* **18** 319–28

[92] Kim Y-T, Hitchcock R W, Bridge M J and Tresco P A 2004 Chronic response of adult rat brain tissue to implants anchored to the skull *Biomaterials* **25** 2229–37

[93] Ledochowitsch P, Tiefenauer R F, Pepin B, Maharbiz M M and Blanche T J 2013 Nanoflex for neural nanopobes *IEEE 17th Int. Solid-State Sensors, Actuators and Microsystems Conf., Transducers (Barcelona, Spain, 16–20 June 2013)* pp 1278–81

[94] Ozawa H, Matsumoto T, Ohashi T, Sato M and Kokubun S 2004 Mechanical properties and function of the spinal pia mater *J. Neurosurgery: Spine* **1** 122–7

[95] Runza M, Pietrabissa R, Mantero S, Albani A, Quaglini V and Contro R 1999 Lumbar dura mater biomechanics: experimental characterization and scanning electron microscopy observations *Anesthesia Analgesia* **88** 1317–21

[96] Kralik J D, Dimitrov D F, Krupa D J, Katz D B, Cohen D and Nicolelis M A 2001 Techniques for long-term multisite neuronal ensemble recordings in behaving animals *Methods* **25** 121–50

[97] Paralikar K J, Lawrence J K and Clement R S 2006 Collagenase-aided insertion of intracortical microelectrode arrays: evaluation of insertion force and chronic recording performance *IEEE Eng. Med. Biol. Soc.* **1** 2958–61

[98] Hsu J M, Rieth L, Normann R A, Tathireddy P and Solzbacher F 2009 Encapsulation of an integrated neural interface device with parylene C *IEEE Trans. Biomed. Eng.* **56** 23–9

[99] McCracken P J, Manduca A, Felmlee J and Ehman R L 2005 Mechanical transient-based magnetic resonance elastography *Magn. Reson. Med.* **53** 628–39

[100] Hosseini N H, Hoffmann R, Kisban S, Stieglitz T, Paul O and Ruther P 2007 Comparative study on the insertion behavior of cerebral microprobes *29th Annual Int. Conf. of the IEEE Eng. Med. Biol. Soc. (Lyon, France, 22–26 August 2007)* 4711–4

[101] Tian C and He J 2005 Monitoring insertion force and electrode impedance during implantation of microwire electrodes *27th Annual Int. Conf. of the IEEE Eng. Med. Biol. Soc. (Shanghai, China, 17–18 January 2006)* **7** 7333–6

[102] Jensen W, Hofmann U and Yoshida K 2003 Assessment of subdural insertion force of single-tine microelectrodes in rat cerebral cortex *25th Annual Int. Conf. of the IEEE Eng. Med. Biol. Soc. (Cancun, Mexico, 17–21 September 2003)* 2168–71

[103] Molloy J A, Ritter R C, Grady M S, Howard M A, Quate E G and Gillies G T 1990 Experimental determination of the force required for insertion of a thermoseed into deep brain tissues *Ann. Biomed. Eng.* **18** 299–313

[104] Howard M A, Abkes B A, Ollendieck M C, Noh M D, Ritter R C and Gillies G T 1999 Measurement of the force required to move a neurosurgical probe through *in vivo* human brain tissue *IEEE Trans. Biomed. Eng.* **46** 891–4

[105] Welkenhuysen M, Andrei A, Ameye L, Eberle W and Nuttin B 2011 Effect of insertion speed on tissue response and insertion mechanics of a chronically implanted silicon-based neural probe *IEEE Trans. Biomed. Eng.* **58** 3250–9

[106] Andrei A, Welkenhuysen M, Nuttin B and Eberle W 2011 A response surface model predicting the *in vivo* insertion behavior of micromachined neural implants *J. Neural Eng.* **9** 016005

[107] Wester B A, Lee R H and LaPlaca M C 2009 Development and characterization of *in vivo* flexible electrodes compatible with large tissue displacements *J. Neural Eng.* **6** 024002

[108] Rousche P J, Pellinen D S, Pivin D P, Williams J C, Vetter R J and Kipke D R 2001 Flexible polyimide-based intracortical electrode arrays with bioactive capability *IEEE Trans. Biomed. Eng.* **48** 361–70

[109] Egert D, Peterson R L and Najafi K 2011 Parylene microprobes with engineered stiffness and shape for improved insertion *16th Int. Solid-State Sensors, Actuators and Microsystems Conf.* pp 198–201

[110] Kim E G, John J K, Tu H, Zheng Q, Loeb J, Zhang J and Xu Y 2014 A hybrid silicon-parylene neural probe with locally flexible regions *Sensors Actuators* B **195** 416–22

[111] Felix S, Shah K, George D, Tolosa V, Tooker A, Sheth H, Delima T and Pannu S 2012 Removable silicon insertion stiffeners for neural probes using polyethylene glycol as a biodissolvable adhesive *Annual Int. Conf. of the IEEE Engineering in Medicine and Biology Society* pp 871–4

[112] Barz F, Ruther P, Takeuchi S and Paul O 2015 Flexible silicon-polymer neural probe rigidified by dissolvable insertion vehicle for high resolution neural recording with improved duration *IEEE MEMS* pp 636–9

[113] Kozai T D Y and Kipke D R 2009 Insertion shuttle with carboxyl terminated self-assembled monolayer coatings for implanting flexible polymer neural probes in the brain *J. Neurosci. Methods* **184** 199–205

[114] Sohal H S, Jackson A, Jackson R, Clowry G J, Vassilevski K, O'Neill A and Baker S N 2014 The sinusoidal probe: a new approach to improve electrode longevity *Frontiers Neuroeng.* **7** 10

[115] Wang Y-H *et al* 2014 Micro-wing and pore design in an implantable FPC-based neural stimulation probe for minimally invasive surgery *IEEE 27th Int. Conf. on Micro Electro Mechanical Systems* pp 861–4

[116] Tamaki S, Matsunaga T, Kuki T, Furusawa Y and Musiake H 2013 Development and evaluation of tube-shaped neural probe with working channel *17th Int. Solid-State Sensors, Actuators and Microsystems Conf., Transducers (Barcelona, Spain, 16–20 June 2013)* pp 864–7

[117] Richter A *et al* 2013 A simple implantation method for flexible, multisite microelectrodes into rat brains *Front. Neuroeng.* **6** 6

[118] Ware T, Simon D, Liu C, Musa T, Vasudevan S, Sloan A, Keefer E W, Rennaker R L and Voit W 2013 Thiol-ene/acrylate substrates for softening intracortical electrodes *J. Biomed. Mater. Res. B* **102** 1–11

[119] Hess A E, Capadona J R, Shanmuganathan K, Hsu L, Rowan S J, Weder C, Tyler D J and Zorman C A 2011 Development of a stimuli-responsive polymer nanocomposite toward biologically optimized, MEMS-based neural probes *J. Micromech. Microeng.* **21** 054009

[120] Ward M A and Georgiou T K 2011 Thermoresponsive polymers for biomedical applications *Polymers* **3** 1215–42

[121] Ware T *et al* 2012 Three-dimensional flexible electronics enabled by shape memory polymer substrates for responsive neural interfaces *Macromol. Mater. Eng.* **297** 1193–202

[122] Capadona J R, Shanmuganathan K, Tyler D J, Rowan S J and Weder C 2008 Stimuli-responsive polymer

nanocomposites inspired by the sea cucumber dermis *Science* **319** 1370–4
[123] Shanmuganathan K, Capadona J R, Rowan S J and Weder C 2010 Bio-inspired mechanically-adaptive nanocomposites derived from cotton cellulose whiskers *J. Mater. Chem.* **20** 180
[124] Harris J P, Capadona J R, Miller R H, Healy B C, Shanmuganathan K, Rowan S J, Weder C and Tyler D J 2011 Mechanically adaptive intracortical implants improve the proximity of neuronal cell bodies *J. Neural Eng.* **8** 066011
[125] Wu F, Im M and Yoon E 2011 A flexible fish-bone-shaped neural probe strengthened by biodegradable silk coating for enhanced biocompatibility *16th Int. Solid-State Sensors, Actuators and Microsystems Conf.,Transducers (Beijing, China, 5–9 June 2011)* pp 966–9
[126] Kato Y, Saito I, Hoshino T, Suzuki T and Mabuchi K 2006 Preliminary study of multichannel flexible neural probes coated with hybrid biodegradable polymer *IEEE Eng. Med. Biol. Mag.* **1** 660–3
[127] Foley C P, Nishimura N, Neeves K B, Schaffer C B and Olbricht W L 2009 Flexible microfluidic devices supported by biodegradable insertion scaffolds for convection-enhanced neural drug delivery *Biomed. Microdevices* **11** 915–24
[128] Stice P, Gilletti A, Panitch A and Muthuswamy J 2007 Thin microelectrodes reduce GFAP expression in the implant site in rodent somatosensory cortex *J. Neural Eng.* **4** 42–53
[129] Gunatillake P A and Adhikari R 2003 Biodegradable synthetic polymers for tissue engineering *Eur. Cells Mater.* **5** 1–16
[130] Nair L S and Laurencin C T 2007 Biodegradable polymers as biomaterials *Prog. Polymer Sci.* **32** 762–98
[131] Ikada Y and Tsuji H 2000 Biodegradable polyesters for medical and ecological applications *Macromol. Rapid Commun.* **21** 117–32
[132] Kim D H and Martin D C 2006 Sustained release of dexamethasone from hydrophilic matrices using PLGA nanoparticles for neural drug delivery *Biomaterials* **27** 3031–7
[133] Athanasiou K A, Niederauer G G and Agrawal C M 1996 Sterilization, toxicity, biocompatibility and clinical applications of polylactic acid/polyglycolic acid copolymers *Biomaterials* **17** 93–102
[134] Holy C E, Cheng C, Davies J E and Shoichet M S 2001 Optimizing the sterilization of PLGA scaffolds for use in tissue engineering *Biomaterials* **22** 25–31
[135] Lo M-C, Wang S, Singh S, Damodaran V B, Kaplan H M, Kohn J, Shreiber D I and Zahn J D 2015 Coating flexible probes with an ultra fast degrading polymer to aid in tissue insertion *Biomed. Microdevices* **17** 34
[136] Lewitus D Y, Smith K L, Shain W, Bolikal D and Kohn J 2011 The fate of ultrafast degrading polymeric implants in the brain *Biomaterials* **32** 5543–50
[137] Lewitus D, Smith K L, Shain W and Kohn J 2011 Ultrafast resorbing polymers for use as carriers for cortical neural probes *Acta Biomater.* **7** 2483–91
[138] Bourke S L and Kohn J 2003 Polymers derived from the amino acid L-tyrosine: Polycarbonates, polyarylates and copolymers with poly(ethylene glycol) *Adv. Drug Deliv. Rev.* **55** 447–66
[139] Lind G, Linsmeier C E, Thelin J and Shouenborg J 2010 Gelatin-embedded electrodes—a novel biocompatible vehicle allowing implantation of highly flexible microelectrodes *J. Neural Eng.* **7** 046005
[140] Grant C A, Brockwell D J, Radford S E and Thomson N H 2009 Tuning the elastic modulus of hydrated collagen fibrils *Biophys. J.* **97** 2985–92
[141] Gorgieva S and Kokol V 2011 Collagen versus gelatine based biomaterials and their biocompatibility: review and perspectives *Biomaterials—Applications for Nanomedicine* pp 17–52
[142] Paige M F, Lin A C and Goh M C 2002 Real-time enzymatic biodegradation of collagen fibrils monitored by atomic force microscopy *Int. Biodeterioration Biodegradation* **50** 1–10
[143] Wiegand C, Abel M, Ruth P, Wilhelms T, Schulze D, Norgauer J and Hipler U-C 2009 Effect of the sterilization method on the performance of collagen Type I on chronic wound parameters *in vitro J. Biomed. Mater. Res.* B **90** 710–9
[144] Ceyssens F, Kuyck K V, Nuttin B and Puers R 2012 Neural implants containing a resorbable chitosan matrix *26th European Conf. on Solid-State Transducers (Krakow, Poland, 9–12 September 2012)* vol 47 pp 688–9
[145] Ceyssens F, van Kuyck K, Velde G V, Welkenhuysen M, Stappers L, Nuttin B and Puers R 2013 Resorbable scaffold based chronic neural electrode arrays *Biomed. Microdevices* **15** 481–93
[146] Ceyssens F, Van Kuyck K, Nuttin B and Puers R 2013 Long term LFP measurements with ultra-fine neural electrodes embedded in porous resorbable carrier *17th Int. Solid-State Sensors, Actuators and Microsystems Conf., Transducers (Barcelona, Spain, 16–20 June 2013)* pp 868–71
[147] Amin K A M and Panhuis M I H 2012 Reinforced materials based on chitosan, TiO2 and Ag composites *Polymers* **4** 590–9
[148] Kim I-Y, Seo S-J, Moon H-S, Yoo M-K, Park I-Y, Kim B-C and Cho C-S 2008 Chitosan and its derivatives for tissue engineering applications *Biotechnol. Adv.* **26** 1–21
[149] Khor E and Lim L Y 2003 Implantable applications of chitin and chitosan *Biomaterials* **24** 2339–49
[150] Shi W *et al* 2012 BDNF blended chitosan scaffolds for human umbilical cord MSC transplants in traumatic brain injury therapy *Biomaterials* **33** 3119–26
[151] Hassler C, Member S, Guy J, Nietzschmann M and Staiger J F 2011 Chronic intracortical implantation of saccharose-coated flexible shaft electrodes into the cortex of rats *33rd Annual Int. Conf. of the IEEE Eng. Med. Biol. Soc. (Boston, MA, 30 August–3 September 2011)* pp 644–7
[152] Jeon M, Cho J, Kim Y K, Jung D, Yoon E-S, Shin S and Cho I-J 2014 Partially flexible MEMS neural probe composed of polyimide and sucrose gel for reducing brain damage during and after implantation *J. Micromech. Microeng.* **24** 025010
[153] Hassler C, Guy J, Nietzschmann M, Plachta D T T, Staiger J F and Stieglitz T 2016 Intracortical polyimide electrodes with a bioresorbable coating *Biomed. Microdevices* **18** 1–12
[154] Mullarney M P, Hancock B C, Carlson G T, Ladipo D D and Langdon B A 2003 The powder flow and compact mechanical properties of sucrose and three high-intensity sweeteners used in chewable tablets *Int. J. Pharmaceutics* **257** 227–36
[155] Barz F, Holzhammer T, Paul O and Ruther P 2013 Novel technology for the in-plane transfer of multiple interconnection lines in 3D neural probes *17th Int. Solid-State Sensors, Actuators and Microsystems Conf., Transducers (Barcelona, Spain, 16–20 June 2013)* pp 884–7
[156] Jee A-Y, Lee H, Lee Y and Lee M 2013 Determination of the elastic modulus of poly(ethylene oxide) using a photoisomerizing dye *Chem. Phys.* **422** 246–50
[157] Nie H-Y, Motomatsu M, Mizutani W and Tokumoto H 1995 Local modification of elastic properties of

polystyrene-polyethyleneoxide blend surface *J. Vac. Sci. Technol.* B **13** 1163–6
[158] Al-Nasassrah M A, Podczeck F and Newton J M 1998 The effect of an increase in chain length on the mechanical properties of polyethylene glycols *Eur. J. Pharmaceutics Biopharmaceutics* **46** 31–8
[159] Bjugstad K B, Lampe K, Kern D S and Mahoney M 2010 Biocompatibility of poly(ethylene glycol)-based hydrogels in the brain: an analysis of the glial response across space and time *J. Biomed. Mater. Res.* A **95** 79–91
[160] Lin C-C and Anseth K S 2009 PEG hydrogels for the controlled release of biomolecules in regenerative medicine *Pharm. Res.* **26** 631–43
[161] Rao L, Zhou H, Li T, Li C and Duan Y Y 2012 Polyethylene glycol-containing polyurethane hydrogel coatings for improving the biocompatibility of neural electrodes *Acta Biomater.* **8** 2233–42
[162] Kim D-H *et al* 2010 Dissolvable films of silk fibroin for ultrathin conformal bio-integrated electronics *Nat. Mater.* **9** 511–7
[163] Tien L W, Wu F, Tang-Schomer M D, Yoon E, Omenetto F G and Kaplan D L 2013 Silk as a multifunctional biomaterial substrate for reduced glial scarring around brain-penetrating electrodes *Adv. Funct. Mater.* **23** 3185–93
[164] Wu F, Tien L, Chen F, Kaplan D, Berke J and Yoon E 2013 A multi-shank silk-backed parylene neural probe for reliable chronic recording *17th Int. Solid-State Sensors, Actuators and Microsystems Conf., Transducers (Barcelona, Spain, 16–20 June 2013)* pp 888–91
[165] Jiang C, Wang X, Gunawidjaja R, Lin Y H, Gupta M K, Kaplan D L, Naik R R and Tsukruk V V 2007 Mechanical properties of robust ultrathin silk fibroin films *Adv. Funct. Mater.* **17** 2229–37
[166] Altman G H, Diaz F, Jakuba C, Calabro T, Horan R L, Chen J, Lu H, Richmond J and Kaplan D L 2003 Silk-based biomaterials *Biomaterials* **24** 401–16
[167] Vepari C and Kaplan D L 2007 Silk as a biomaterial *Prog. Polymer Sci.* **32** 991–1007
[168] Jin H-J, Park J, Karageorgiou V, Kim U-J, Valluzzi R, Cebe P and Kaplan D L 2005 Water-stable silk films with reduced β-sheet content *Adv. Funct. Mater.* **15** 1241–7
[169] Lin Y-C, Ramadan M, Hronik-Tupaj M, Kaplan D L, Philips B J, Sivak W, Rubin J P and Marra K G 2011 Spatially controlled delivery of neurotrophic factors in silk fibroin-based nerve conduits for peripheral nerve repair *Ann. Plast. Surg.* **67** 147–55
[170] Uebersax L, Mattotti M, Papaloïzos M, Merkle H P, Gander B and Meinel L 2007 Silk fibroin matrices for the controlled release of nerve growth factor (NGF) *Biomaterials* **28** 4449–60
[171] Hofmann S, Stok K S, Kohler T, Meinel A J and Müller R 2014 Effect of sterilization on structural and material properties of 3D silk fibroin scaffolds *Acta Biomater.* **10** 308–17
[172] Yucel T, Lovett M L and Kaplan D L 2014 Silk-based biomaterials for sustained drug delivery *J. Control. Release* **190** 381–97
[173] Horan R L, Antle K, Collette A L, Wang Y, Huang J, Moreau J E, Volloch V, Kaplan D L and Altman G H 2005 *In vitro* degradation of silk fibroin *Biomaterials* **26** 3385–93
[174] Gomes M E and Reis R L 2004 Biodegradable polymers and composites in biomedical applocations: from catgut to tissue engineering *Int. Mater. Rev.* **495** 261–73
[175] Kozai T D Y, Gugel Z, Li X, Gilgunn P J, Khilwani R, Ozdoganlar O B, Fedder G K, Weber D J and Cui X T 2014 Chronic tissue response to carboxymethyl cellulose based dissolvable insertion needle for ultra-small neural probes *Biomaterials* **35** 9255–68
[176] Das D, Zhang Z, Winkler T, Mour M, Gunter C I, Morlock M M, Machens H G and Schilling A F 2011 Bioresorption and degradation of biomaterials *Tissue Engineering III: Cell - Surface Interactions for Tissue Culture. Advances in Biochemical Engineering Biotechnology* vol 126, ed C Kasper, F Witte, R Pörtner (Berlin: Springer)
[177] Cooperman L and Michaeli D 1984 The immunogenicity of injectable collagen: a 1-year prospective study *J. Am. Acad. Dermatol.* **10** 638–46
[178] Booth A F 1999 *Sterilization of Medical Devices* (Boca Raton, FL: CRC Press)
[179] Yagi S, Yamagiwa S, Kubota Y, Sawahata H, Numano R, Imashioya T, Oi H, Ishida M and Kawano T 2015 Dissolvable base scaffolds allow tissue penetration of high-aspect-ratio flexible microneedles *Adv. Healthcare Mater.* **4** 1949–55
[180] Patel P R, Na K, Zhang H, Kozai T D Y, Kotov N A, Yoon E and Chestek C A 2015 Insertion of linear 8.4 μm diameter 16 channel carbon fiber electrode arrays for single unit recordings *J. Neural Eng.* **12** 046009
[181] Xu H, Weltman A, Hsiao M-C, Scholten K, Meng E, Berger T W and Song D 2016 A flexible parylene probe for *in vivo* recordings from multiple subregions of the rat hippocampus *IEEE 38th EMBC Conf.* pp 2806–9
[182] Fernandez E, Greger B, House P A, Aranda I, Botella C, Albisua J, Soto-Sanchez C, Alfaro A and Normann R A 2014 Acute human brain responses to intracortical microelectrode arrays: challenges and future prospects *Front. Neuroeng.* **7** 24
[183] Edell D J, Toi V V, McNeil V M and Clark L D 1992 Factors influencing the biocompatibility of insertable silicon microshafts in cerebral cortex *IEEE Trans. Bio-Med. Eng.* **39** 635–43
[184] Rennaker R L, Street S, Ruyle A M and Sloan A M 2005 A comparison of chronic multi-channel cortical implantation techniques: manual versus mechanical insertion *J. Neurosci. Methods* **142** 169–76
[185] Fekete Z, Németh A, Márton G, Ulbert I and Pongrácz A 2015 Experimental study on the mechanical interaction between silicon neural microprobes and rat dura mater during insertion *J. Mater. Sci.: Mater. Med.* **26** 70
[186] Szarowski D H, Andersen M D, Retterer S, Spence A J, Isaacson M, Craighead H G, Turner J N and Shain W 2003 Brain responses to micro-machined silicon devices *Brain Res.* **983** 23–35
[187] Ward M P, Rajdev P, Ellison C and Irazoqui P P 2009 Toward a comparison of microelectrodes for acute and chronic recordings *Brain Res.* **1282** 183–200
[188] Prasad A, Xue Q-S, Dieme R, Sankar V, Mayrand R C, Nishida T, Streit W J and Sanchez J C 2014 Abiotic-biotic characterization of Pt/Ir microelectrode arrays in chronic implants *Front. Neuroeng.* **7** 2
[189] Liu H, Zhou Y, Chen S, Bu M, Xin J and Li S 2013 Current sustained delivery strategies for the design of local neurotrophic factors in treatment of neurological disorders *Asian J. Pharm. Sci.* **8** 269–77
[190] Johnson P J, Skornia S L, Stabenfeldt S E and Willits R K 2008 Maintaining bioactivity of NGF for controlled release from PLGA using PEG *J. Biomed. Mater. Res.* A **86** 420–7
[191] Potter K A, Jorfi M, Householder K T, Foster E J, Weder C and Capadona J R 2014 Curcumin-releasing mechanically adaptive intracortical implants improve the proximal neuronal density and blood-brain barrier stability *Acta Biomater.* **10** 2209–22

[192] Green R A, Lim K S, Henderson W C, Hassarati R T, Martens P J, Lovell N H and Poole-Warren L A 2013 Living electrodes: tissue engineering the neural interface *35th Annual Int. Conf. of the IEEE Eng. Med. Biol. Soc. (Osaka, Japan, 3–7 July 2013)* **2013** 6957–60

[193] Richter A, Kruse C, Moser A, Hofmann U G and Danner S 2011 Cellular modulation of polymeric device surfaces: promise of adult stem cells for neuro-prosthetics *Front. Neurosci.* **5** 1–10

[194] Purcell E K, Seymour J P, Yandamuri S and Kipke D R 2009 *In vivo* evaluation fo a neural stem cell-seeded prosthesis *J. Neural Eng.* **6** 130–4

[195] Kozai T D Y, Catt K, Li X, Gugel Z V, Olafsson V T, Vazquez A L and Cui X T 2014 Biomaterials mechanical failure modes of chronically implanted planar silicon-based neural probes for laminar recording *Biomaterials* **37** 25–39

[196] Kato Y, Nishino M, Saito I, Suzuki T and Mabuchi K 2006 Flexible intracortical neural probe with biodegradable polymer for delivering bioactive components *Int. Conf. on Microtechnologies in Medicine and Biology* pp 143–6

[197] Zhu W, O'Brien C, O'Brien J R and Zhang L G 2014 3D nano/microfabrication techniques and nanobiomaterials for neural tissue regeneration *Nanomedicine* **9** 859–75

[198] Lee Y-S and Livingston Arinzeh T 2011 Electrospun nanofibrous materials for neural tissue engineering *Polymers* **3** 413–26

[199] Yang F, Murugan R, Wang S and Ramakrishna S 2005 Electrospinning of nano/micro scale poly(l-lactic acid) aligned fibers and their potential in neural tissue engineering *Biomaterials* **26** 2603–10

[200] Dinis T M, Vidal G, Jose R R, Vigneron P, Bresson D, Fitzpatrick V, Marin F, Kaplan D L and Egles C 2014 Complementary effects of two growth factors in multifunctionalized silk nanofibers for nerve reconstruction *PLoS One* **9** e109770

[201] Almeida C R, Serra T, Oliveira M I, Planell J A, Barbosa M A and Navarro M 2014 Impact of 3D printed PLA- and chitosan-based scaffolds on human monocyte/macrophage responses: unraveling the effect of 3D structures on inflammation *Acta Biomater.* **10** 613–22

[202] Chia H N and Wu B M 2015 Recent advances in 3D printing of biomaterials *J. Biol. Eng.* **9** 4

[203] Tao H, Marelli B, Yang M, An B, Onses M S, Rogers J A, Kaplan D L and Omenetto F G 2015 Inkjet printing of regenerated silk fibroin: from printable forms to printable functions *Adv. Mater.* **27** 4273–9

[204] Vozzi G, Flaim C, Ahluwalia A and Bhatia S 2003 Fabrication of PLGA scaffolds using soft lithography and microsyringe deposition *Biomaterials* **24** 2533–40

[205] Ho M H, Kuo P Y, Hsieh H J, Hsien T Y, Hou L T, Lai J Y and Wang D M 2004 Preparation of porous scaffolds by using freeze-extraction and freeze-gelation methods *Biomaterials* **25** 129–38